

Enhancing Adsorption Capacity of a Kaolinite Mineral through Acid Activation and Manual Blending with a 2:1 Clay

T. O. Abu^{1*}, H. I. Adegoke², E. O. Odebunmi³, M. A. Shehzad⁴

¹Department of Industrial Chemistry, University of Ilorin, Ilorin, Nigeria

²Department of Chemistry, University of Ilorin, Ilorin, Nigeria

³Department of Chemistry, Thomas Adewumi University, Oko, Nigeria

⁴Department of Material Science and Engineering, Northwestern University, Evanston, Illinois 60208, United States



ABSTRACT: The efficiencies of raw and modified kaolinite mineral in removing selected heavy metal ions from their respective aqueous solutions were investigated. The mineral was modified through two different methods; i) activation with HNO₃, H₂SO₄, H₃PO₄, CH₃COOH and C₂H₂O₄ acids to form NK, SK, PK, AK and OK acid activated clays respectively and ii) preparations of 3:1 and 1:1 Kaolinite: Bentonite blends to form UBK and EBK composites respectively through manual blending. The adsorbents were characterized by X-ray Diffraction (XRD), Scanning Electron Microscopy (SEM), Fourier Transform Infra-Red Spectroscopy (FTIR) and Brunauer Emmett Teller (BET) analysis for surface area determination. The surface area increased in some of the modified clays from 114.9457 m²/g (RK) to 288.685 m²/g (EBK), 205.92 m²/g (UBK), 162.227 m²/g (NK), 151.335 m²/g (SK), and 115.837 m²/g (OK) but reduced to 113.872 m²/g (PK) and 112.865 m²/g (AK) after modification. Adsorption studies were subsequently conducted out to remove Pb²⁺, Cd²⁺ and Ni²⁺ ions from synthetic solutions. Pb²⁺ was found to be most removed (383.5 mg g⁻¹ (RK), 591.13 mg g⁻¹ (EBK), 576.61 mg g⁻¹ (UBK), 475 mg g⁻¹ (NK), 450 mg g⁻¹ (SK), and 425 mg g⁻¹ (PK), 375 mg g⁻¹ (OK) and 375 mg g⁻¹ (AK)) with highest removals on the composites.

KEYWORDS: Kaolinite, Bentonite, Composites, Adsorption, Heavy metals

[Received. Jan. 1, 2024; Revised Feb 2, 2024; Accepted Feb 13, 2024]

Print ISSN: 0189-9546 | Online ISSN: 2437-2110

I. INTRODUCTION

Industrial wastewaters have been found to contain heavy metal ions such as lead, cadmium, chromium and nickel amongst others (Berihun and Solomon, 2017, Huang *et al.*, 2020, Dim *et al.*, 2021, Aziz *et al.*, 2023). The metals bioaccumulate because of their non-susceptibility to biodegradation and also exhibit carcinogenic tendencies causing them to be considered as hazardous pollutants. Thus, their removal from industrial wastewaters before their discharge into the water environment is highly necessary (Khalifa *et al.*, 2020, Balali-Mood *et al.*, 2021, Razzak *et al.*, 2022). To accomplish this feat, various wastewater treatment techniques have been evaluated out of which adsorption is proposed to be the most preferable due to reasonable costs of design and operation (Uddin, 2017, Dim *et al.*, 2021, Malima *et al.*, 2021).

Activated carbon remains the choice adsorbent for adsorption of pollutants from wastewaters but the costly methods of operation and regeneration challenges necessitated the current growth spurt in the search for alternative cheaper adsorbents (Crini *et al.*, 2019, Almeida-Naranjo *et al.*, 2023). Several materials have been evaluated as suitable alternatives but most of them have been discovered to be accompanied by challenges such as low adsorption capacities, premature

fouling, short half-life among others all of which have made their industrial use for remediation purposes impractical (Aragaw and Bogale, 2021). All of these justify the increasing attention focused on natural minerals especially clays because of their local availability, natural abundance, and modification potentials (Ngulube *et al.*, 2017, Li *et al.*, 2020)

Adsorption of pollutants on natural clay minerals have been successfully carried out and it has also been demonstrated to be enhanced by the modification of the clay surfaces (Mudzielwana *et al.*, 2019). Modified clays are however not without their own shortcomings, but acid activated clays have been found to provide the most advantages associated with modification. This is due to their ease and low cost of production (Özcan and Özcan, 2004, Mohammed-Azizi *et al.*, 2013, Lawal *et al.*, 2020).

Kaolinite clay, being a 1:1 mineral has mostly been reported in literature to possess lower capabilities than 2:1 clay minerals in wastewater treatments and to give better performance in its raw than the activated form (Bhattacharyya and Gupta, 2008). However, Kaolin deposits are reported to be widespread throughout Nigeria such that most states in the country have at least one known deposit which makes it to be easily accessible (Badmus and Olatinsu, 2009, Adeniyi *et al.*, 2020). Thus, it is necessary to find a way of improving its abilities as an adsorbent through simple and practical methods

*Corresponding author: abu.to@unilorin.edu.ng

such as acid activation or formation of composite with 2:1 mineral that has higher adsorptive abilities.

In this study, Kaolinite mineral was purified through sedimentation after which some purified samples were modified with (0.1M) acetic, oxalic, nitric, sulphuric and phosphoric, acids. Some parts of the clay were also used to form 3:1 and 1:1 Kaolinite:Bentonite composites with Bentonite mineral through manual blending of both. The raw as well as modified clays were characterized by Brunauer Emmett Teller (BET) surface area analysis, Fourier Transform Infra-red (FTIR), X-ray Diffractogram (XRD), and Scanning Electron Microscope (SEM). Preliminary experiments were conducted on the raw clay to establish optimum conditions for the removal of Pb^{2+} , Cd^{2+} and Ni^{2+} ions from their respective aqueous solutions. The optimum operating conditions obtained were used for subsequent evaluations on the modified clays.

II. THEORITICAL ANALYSIS

A. Adsorption Isotherms

The experimental data was tested with different adsorption isotherm models to determine the maximum adsorption capacities of the Kaolinite and understand the relationship between the adsorbent and adsorbate at equilibrium (Akpomie and Dawodu, 2016, Pathania *et al*, 2017, Omer *et al*, 2018). The data was fitted into Langmuir, Freundlich, Dubinin-Radushkevich (DBR) and Fowler-Guggenheim (FG) models using the linearized forms of their equations as presented in Eqns. 1 to 4 respectively:

$$\frac{C_e}{q_e} = \frac{1}{K_L q_m} + \frac{1}{q_m} (C_e) \quad (1)$$

$$\ln q_e = \ln K_F + \frac{1}{n} (\ln C_e) \quad (2)$$

$$\ln q_e = \ln q_m - k_{ads} \varepsilon^2 \quad (3)$$

$$\ln \left[\frac{C_e (1-\theta)}{\theta} \right] = -\ln K_{FG} + 2W\theta \left(\frac{1}{RT} \right) \quad (4)$$

Where q_e and C_e are the solid phase concentration ($mg\ g^{-1}$) and equilibrium concentration of the metal ions ($mg\ L^{-1}$) respectively, q_m is the maximum adsorption capacity ($mg\ g^{-1}$) while K_L ($L\ mg^{-1}$) is an empirical Langmuir constant associated with the affinity of the binding site. In Eqn. (2), K_F and n are Freundlich constants related to adsorption capacity and heterogeneity of sorption respectively. In the DBR linearized equation, ε denotes the Polanyi potential and is given as $[RT \ln(1 + 1/C_e)]$, q_m is the theoretical saturation capacity ($mg\ g^{-1}$) and k_{ads} is a constant related to mean free energy of adsorption per mole of the adsorbate ($mol^2/k\ J^2$) (Hamdaoui and Naffrechoux, 2007; Foo and Hameed, 2010, Bahl *et al*, 2012, Nordin *et al.*, 2020, Nandiyanto, 2020). For FG isotherm (Eqn. 4), the values $\ln [(C_e (1-\theta))/\theta]$ were plotted against θ and the values of W (the interaction energy between adsorbed molecules $kJmol^{-1}$ and K_{FG} (Fowler-Guggenheim equilibrium adsorption constant ($L\ mg^{-1}$)) were determined.

B. Kinetics Studies of Adsorption Data

Kinetic modelling of the adsorption data was accomplished using pseudo first order, pseudo second order, and elovich models through the appropriate plots to determine the values of important kinetic parameters. The model whose

regression coefficient R^2 was closest to unity and whose experimental values correlated closely to calculated parameters was used to determine the controlling mechanism of the sorption process (Sukpreabprom *et al.*, 2014, Akpomie and Dawodu, 2016, Pathania *et al.*, 2017, Omer *et al.*, 2018).

1) Pseudo first order model

The linearized Lagergren's equation was used to test for pseudo first order kinetics:

$$\log(q_e - q_t) = \log q_e - \frac{k_1 t}{2.303} \quad (5)$$

$$\frac{t}{q_t} = \frac{1}{k_2 q_e^2} + \frac{t}{q_e} \quad (6)$$

$$q_t = \frac{1}{\beta} \ln(\alpha\beta) + \frac{1}{\beta} \ln t. \quad (7)$$

$$q_t = k_{id} t_{1/2} + C_i \quad (8)$$

Where, k_1 and k_2 are the pseudo first and pseudo second order rate constants (min^{-1}), k_{id} is the intraparticle diffusion rate constant, q_t and q_e are amounts of adsorbates adsorbed at time t and equilibrium respectively ($mg\ g^{-1}$) while α and β are constants that represent the initial adsorption rate ($mg\ min\ g^{-1}$) as well as the extent of surface coverage ($g\ mg^{-1}$). (Abechi *et al.*, 2011, Boparai *et al.*, 2011).

2) Thermodynamic Studies

Thermodynamic parameters such as changes in free energy change (ΔG), enthalpy (ΔH) and entropy (ΔS) were estimated from the data using the Eqns. 9-12 (Boparai *et al*, 2011, Al-Anber 2011):

$$\Delta G = -RT \ln K \quad (9)$$

$$\Delta G = \Delta H - T\Delta S \quad (10)$$

Substitution of equation 9 in to 10 gives the vant' Hoff equation (Levine, 2009; Omer *et al* 2018):

$$\ln K = \frac{\Delta S}{R} - \frac{\Delta H}{RT} \quad (11)$$

K was calculated as follows:

$$K = \frac{q_e}{C_e} \times M_{adsorbate} \times C \quad (12)$$

In Eqn. 12, M is the molecular weight of the adsorbed species, and C is the concentration of the solution (Omer *et al* (2018)). The plot of $\ln K$ against $1/T$ at the different temperatures enabled the determination of the thermodynamic parameters (Sukpreabprom *et al.*, (2014), Akpomie and Dawodu (2016), Pathania *et al.*, (2017), Omer *et al.*, (2018)).

III. MATERIALS AND METHODS/METHODOLOGY/EXPERIMENTAL PROCEDURE

A. Materials

The 2:1 clay mineral used in the study was Bentonite and it was obtained from Afuze deposit, Edo State while the kaolinite was sourced from Share, Kwara state, Nigeria. The chemical reagents that were used include: Cadmium sulphate ($CdSO_4 \cdot 8H_2O$; Molecular weight (MW); 208.47g mol^{-1} , 99.99%); Lead nitrate ($Pb(NO_3)_2$; MW; 331.21g mol^{-1} , 99.0%) Nickel sulphate ($NiSO_4 \cdot 6H_2O$; MW; 154.76 g mol^{-1} , 99.99%); Nitric acid (HNO_3 ; MW; 63.01 g mol^{-1} , 90%); Phosphoric acid (MW ; 98.00 g mol^{-1} , 85%), Hydrochloric acid (MW; 36.46 g mol^{-1} , 97%), Sodium hydroxide (MW; 40.0 g mol^{-1} , 98%); Acetic acid (MW: 60.05g mol^{-1} , 98%) and

Oxalic acid (MW; 90.03 g mol⁻¹, 85%). All reagents were of analytical grade and obtained from BDH Limited, England and Merck, Germany.

B. Experimental Procedure

1) Purification of Kaolinite Clay Mineral

A purification method previously described (Ho *et al.*, 2001; Bhatt *et al.*, 2012) was adopted and modified. It entailed the soaking of 10g of clay in 500 ml of de-ionized water in a 5 L cylindrical plastic container and allowing the resulting suspension to stay undisturbed for 24 hrs. The mixture was subsequently subjected manual stirring for 30 min and left to equilibrate for additional 4 hrs for sedimentation of impurities to occur. The pure clay was separated through careful decantation and subsequent centrifugation using (KUBOTA-6500) at 4000 rpm for 20 min. The wet recovered clay was dried at 80 °C, ground, labelled and stored in airtight sample bottles. The purification method was repeated severally until considerable quantity was successfully purified.

2) Acid Modification

An acid-activation method earlier described (Özcan and Özcan, 2004, Akpomie and Dawodu, 2016) was modified and adopted. A 250 ml of 0.1 M acid was added to 50 g of purified clay in a 500 ml beaker and magnetically stirred for 30 min. The wet acid modified clay was recovered through the same process as the wet purified form earlier described. The clay was subsequently washed thoroughly with de-ionized water until pH 7 was attained. The moist acid-activated clay was dried in an oven at 105 °C for 2 hrs, appropriately labelled and stored.

3) Preparation of Composites of Kaolinite and Bentonite Minerals

A method already described in literature (Daniel-Mkpume *et al.*, 2011; Edoziuno *et al.*, 2016) was modified and used for the preparation of the clay composites. Appropriate amounts of the purified clays to obtain 25:75% and 50:50% composites of Bentonite: Kaolinite mixtures were weighed into two separate 250 ml beakers. Just enough de-ionized water to make slurries was added in each after which the mixtures were stirred rigorously until homogeneity was achieved. This was followed by drying in the oven at 120 °C for 2 hrs after which the samples were grinded and kept in air-tight bottle.

4) Characterization of raw and modified clays

The mineral constituents of the different clay samples were analyzed by measurements using a multipurpose Bruker D8-Advanced X-ray diffractometer with continuous operations of θ - θ scan locked in coupled mode with Cu-K _{α} radiation at i-Themba Labs, South Africa. The SEM/EDX analysis was carried out using Zeiss merlin Microscope at Massachusetts Institute of Technology (MIT), USA while the surface of the Bentonite clay was imaged by Hitachi SU 8230, model Oxford LINK ISIS at Georgia Institute of Technology, (USA). Fourier Transform Infrared (FTIR) spectra were generated with Shimadzu IR Affinity-1S spectrophotometer through mull technique at the University of Cape Town, South Africa. The surface areas of the adsorbents were estimated via

Nitrogen adsorption/desorption isotherms measurements at -196 °C on a Micromeritics Tristar 3020 Porosimeter also at the University of Cape Town, South Africa. The total specific surface area (S_{BET}) was determined by the Brunauer-Emmett-Teller (BET) method while the t-plot method was used for the determination of the micropore volume. The total pore volume was calculated at the relative pressure p/p_0 of 0.97 while the pore size distribution was evaluated through the Barrett-Joyner-Halenda (BJH) method.

5) Adsorption Analysis

Stock solutions of the heavy metal ions were prepared through the dissolution of required amount of respective metal salt (Pb(NO₃)₂, NiSO₄ · 6H₂O, CdSO₄ · 8H₂O.) in appropriate volume of deionized water. Subsequently, a 100 ml of varying concentrations (10-250 mg L⁻¹) of metal solution was introduced into 6 different 250 ml conical flasks and pH adjustments (2 to 4.5 for Pb and 2-7 for Ni and Cd) of the solutions were achieved by dropwise addition of dil. nitric acid (HNO₃) and sodium hydroxide (NaOH) when necessary. A 40 mg of raw kaolinite clay was added into each flask after which they were placed in a rotary shaker at 250 rpm at varying conditions of temperature 30 – 60 °C, and time (10 min – 3.5h). At the end of each time interval, the contents of the flasks were centrifuged at 3000 rpm for 20 min and then filtered. The residual concentrations of the metals in the supernatant solutions were determined by Atomic Absorption Spectroscopy using a Buck 200 spectrophotometer at ROTAS Soil Lab Limited, Ibadan, Nigeria.

The amounts of the metal ions adsorbed were determined using Eqn. (13):

$$q_e = \frac{C_0 - C_e}{m} \times V \quad (13)$$

Where; q_e is the quantity of metal adsorbed (mg g⁻¹).

C_0 is the initial concentration of the metal in the aqueous solution (mg L⁻¹)

C_e is the concentration of the ions at equilibrium (mg L⁻¹)

m is the mass of the adsorbent (g)

V is the volume of metal solution used (L)

IV. RESULTS AND DISCUSSION

A. Characterization of raw and modified adsorbents

1) Results of XRD Analysis

The XRD spectrum in Figure 1a confirms the identity of the raw kaolinite mineral by identifying peaks at 2θ positions (12.34, 19.82, 24.8, 38.38 and 61.96) (Kumar and Lingfa, (2020); Moretti *et al.*, 2020). It also suggests high purity of the clay as Kaolinite is the only identified crystalline phase in the sample indicating the absence of other crystalline phases like quartz and mica (Hai *et al.*, 2015).

It can be observed from Figure 1b that the acid-activated kaolinites retained the structure and crystallinity of the raw clay with insignificant lowering of intensities of the assigned peaks. This implies that de-crystallization of the clay during acid treatment occurred which is a confirmation of the interaction of the acids with the clay surface (Novakovic *et al.*, 2008). Decline in intensity has previously been reported to be

greatly influenced by the strength of the acid (Kumar *et al.*, 2013) and this was also the case in this study as the trend was found to be SK > NK > PK ~ OK > AK.

The typical characteristics of bentonite as a 2:1 mineral to naturally occur with associated minerals is represented by its XRD spectrum in Figure 1c. The composition of the clay includes dominant phases of sodium montmorillonite (Na-Bentonite) at ($2\theta = 8.47, 19.79, 34.95, 54.27, 62.13$ and 71.15), kaolinite at ($2\theta = 12.3, 19.82, 38.38$ and 61.96) and quartz at ($2\theta = 21, 26.58, 39.38, 50, 51$ & 60). It also contains trace amounts of goethite, microcline as and albite high. Quartz is a common impurity found in clay minerals (Olise *et al.*, 2018, Ihekwe *et al.*, 2020). As evident from Figure 1d, the peaks of the raw kaolinite mineral remain unchanged in U-BK having higher intensities for kaolinite peaks but lower for quartz as well as the montmorillonite peaks, but the peaks are narrower in E-BK. Nontronite, and other associated minerals were also found in E-BK while they are absent in U-BK probably due to the higher amount of the 2:1 mineral in the former. The presence of these minerals might not be detrimental to the adsorption characteristics of the clay composites as adsorption studies have been carried out successfully on some of them especially nontronite (Gupta *et al.*, 2006, Guerra *et al.*, 2016, Ye and Fu, 2019) and goethite (Adegoke *et al.*, 2014, Adebayo *et al.*, 2020).

shapes with partial aggregation in some cases. Thus, acid treatment facilitated the formation of lower sized particles on the surface resulting into increased surface area and thus its potential affinity for cation uptake. Similar findings have previously been reported (Hooshiar *et al.*, 2012, Hai *et al.*, 2015 and Ihekwe *et al.*, 2020). The significant differences in the surfaces of the two raw clay minerals and their composites are also evident from Figure 2a. For instance, the surface of U-BK exhibits mild crystallinity and dispersion of flake-like particles (probably contribution from the kaolinite fraction) on larger sized particles of bentonite. The SEM image of E-BK showed particles aggregated together to form larger fluffy lumps with mild dispersion that disallow the proper identification of their shapes as well as sizes. However, U-BK seems to exhibit more porosity than E-BK and this is probably due to the lower amount of bentonite present in the composite. These findings are similar to earlier reports (Novakovic *et al.*, 2008), Mukhopadhyay *et al.*, 2017, Elgamouz *et al.*, 2019).

3) Fourier Transform Infrared Spectroscopy Analysis Results

The spectrum of the raw Kaolinite is shown in Figure 3a from which the functional groups present were identified. The absorption bands at $3687.90, 3622.32$ and 3618.46 cm^{-1} correspond to the inner surface $-\text{OH}$ stretching vibrations

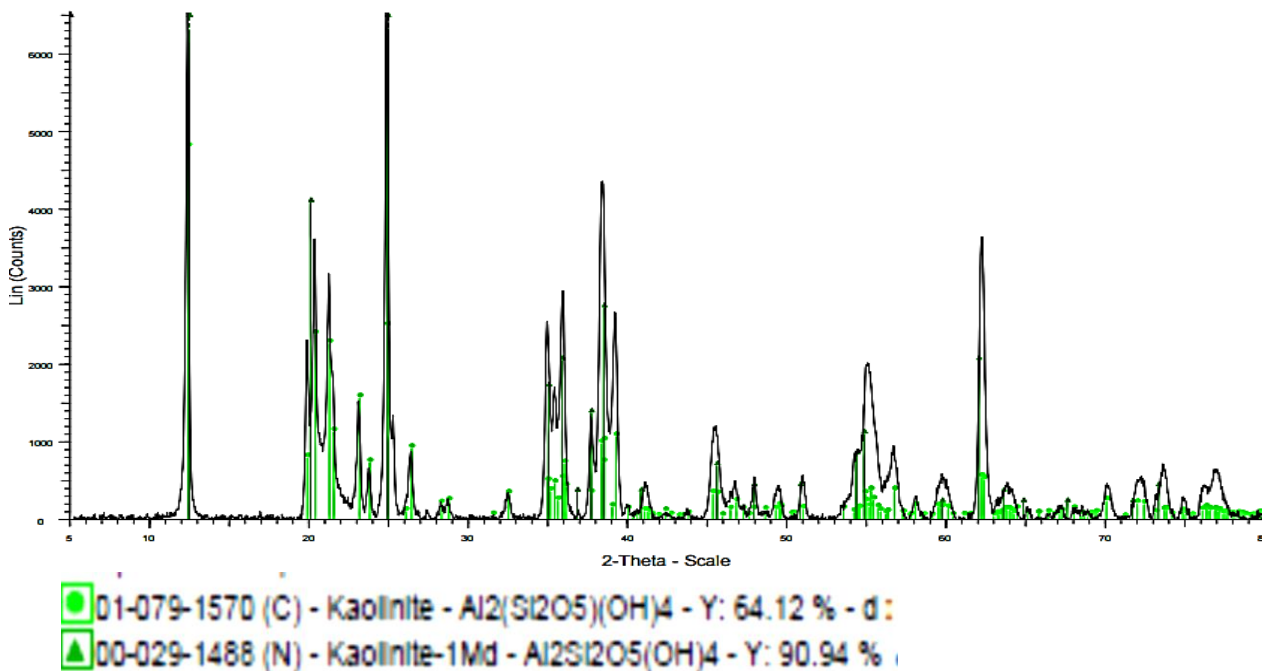


Figure 1a: XRD spectrum of RK

2) Scanning electron microscopy (SEM) results

The surface of the raw kaolinite mineral as shown in Figure 2a shows the aggregation of flake-shaped particles of the clay into clusters that formed a giant aggregate perforated with large pores. However, the SEM images of the modified clays show that the lumped structure of the raw clay had been broken down into different forms depending on the type of modification. The surfaces of the acid-activated clays generally show non-uniform sized porous particles of different

specific to Kaolinite minerals and further affirms the clay as kaolinite (Sdiri *et al.*, 2011, Bukalo *et al.*, 2017, Alshameri *et al.*, 2018, Ihekwe *et al.*, 2020). The $\text{Al}-\text{Al}-\text{OH}$ and $\text{Si}-\text{O}-\text{Si}$ stretching vibrations are suggested by absorption bands at $1006.84, 1026.13$ and 1114.86 cm^{-1} and 914.26 and 790.81 cm^{-1} (octahedral sheet) respectively (Bertagnolli and da Silva (2012); Al-Ashameri *et al.*, 2018, Unuabonah *et al.*, 2008, Madejova *et al.*, 2002 and Panda *et al.*, 2010). The absorption

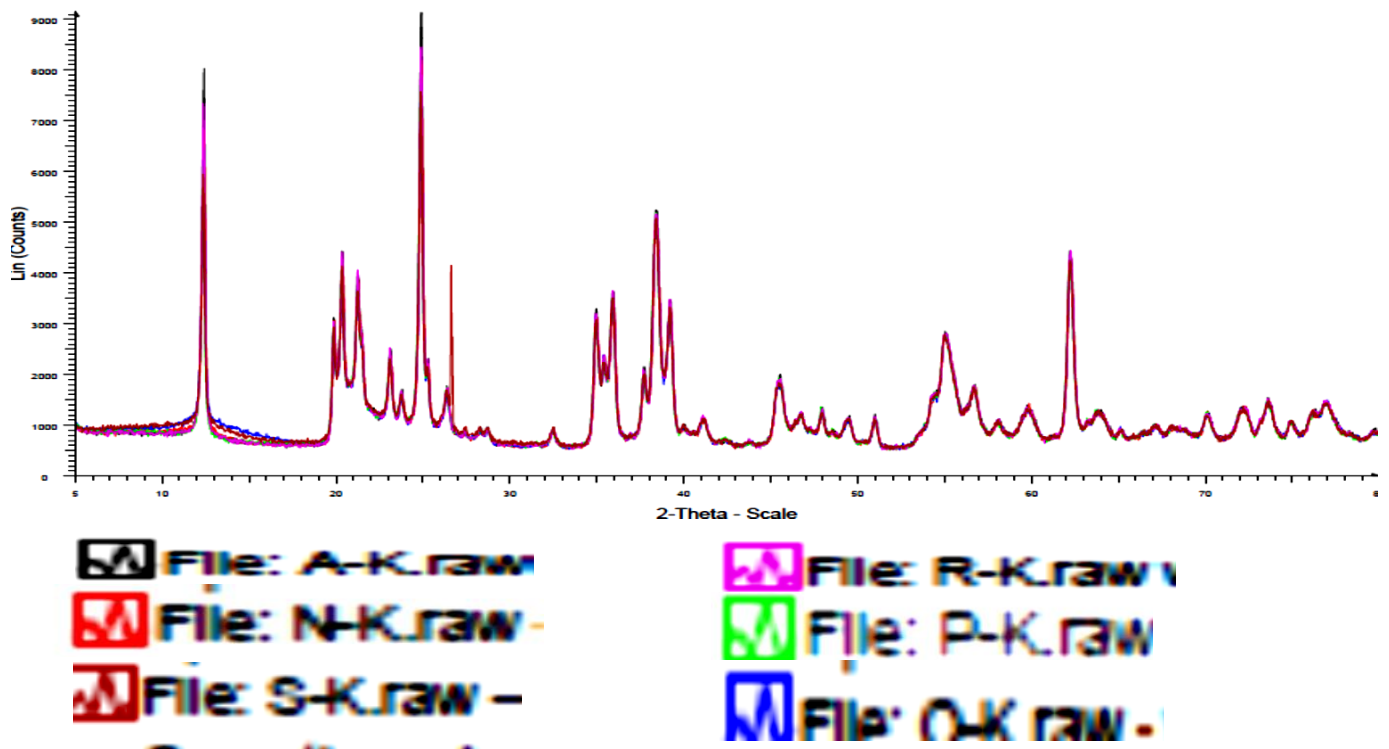


Figure 1b Comparison of the raw and acid-activated clays' XRD spectra

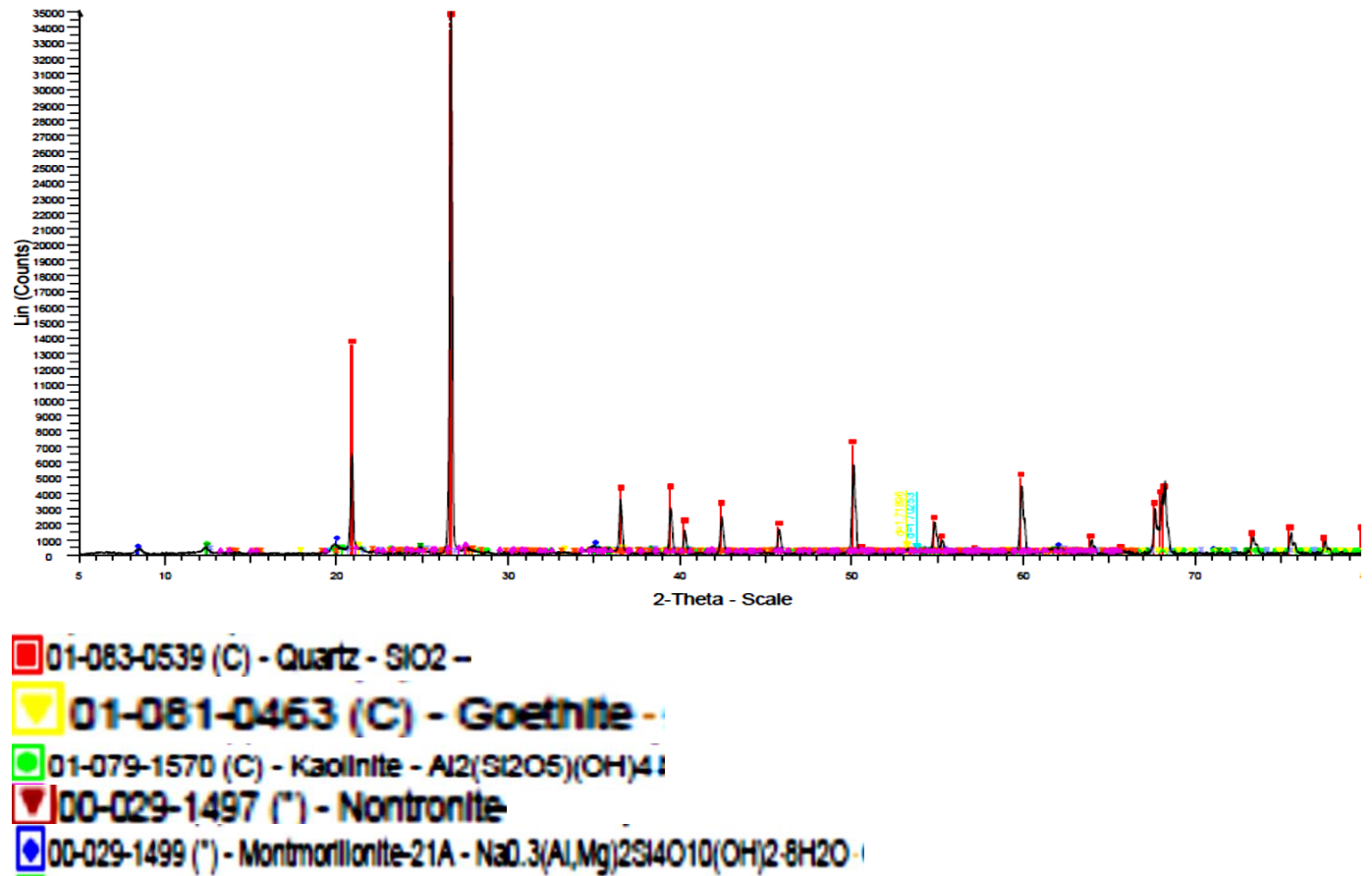


Figure 1c: XRD spectrum of raw Bentonite (RB)

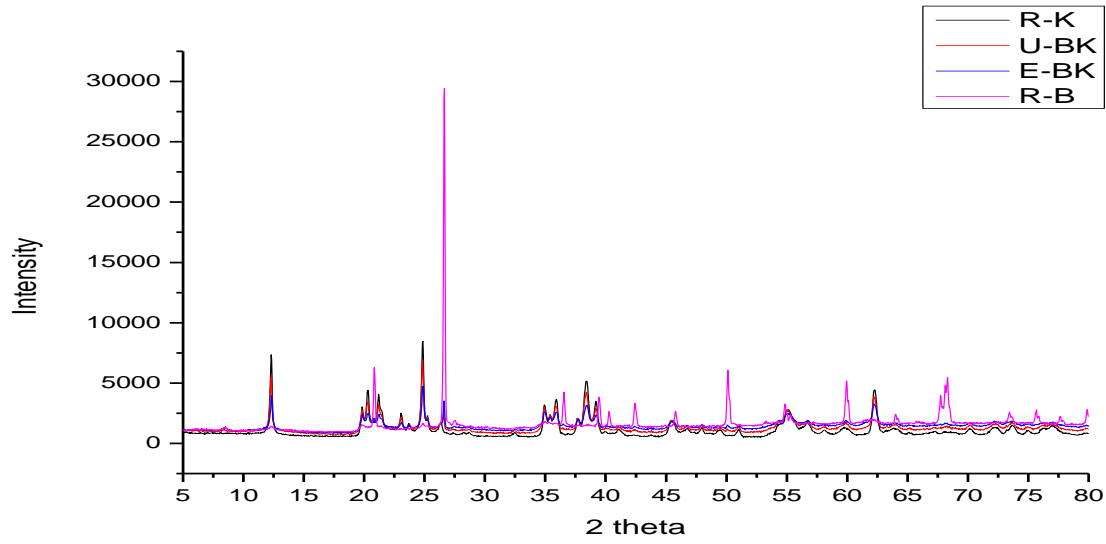


Figure 1d: Compared view of the XRD spectra of the raw clays and composites

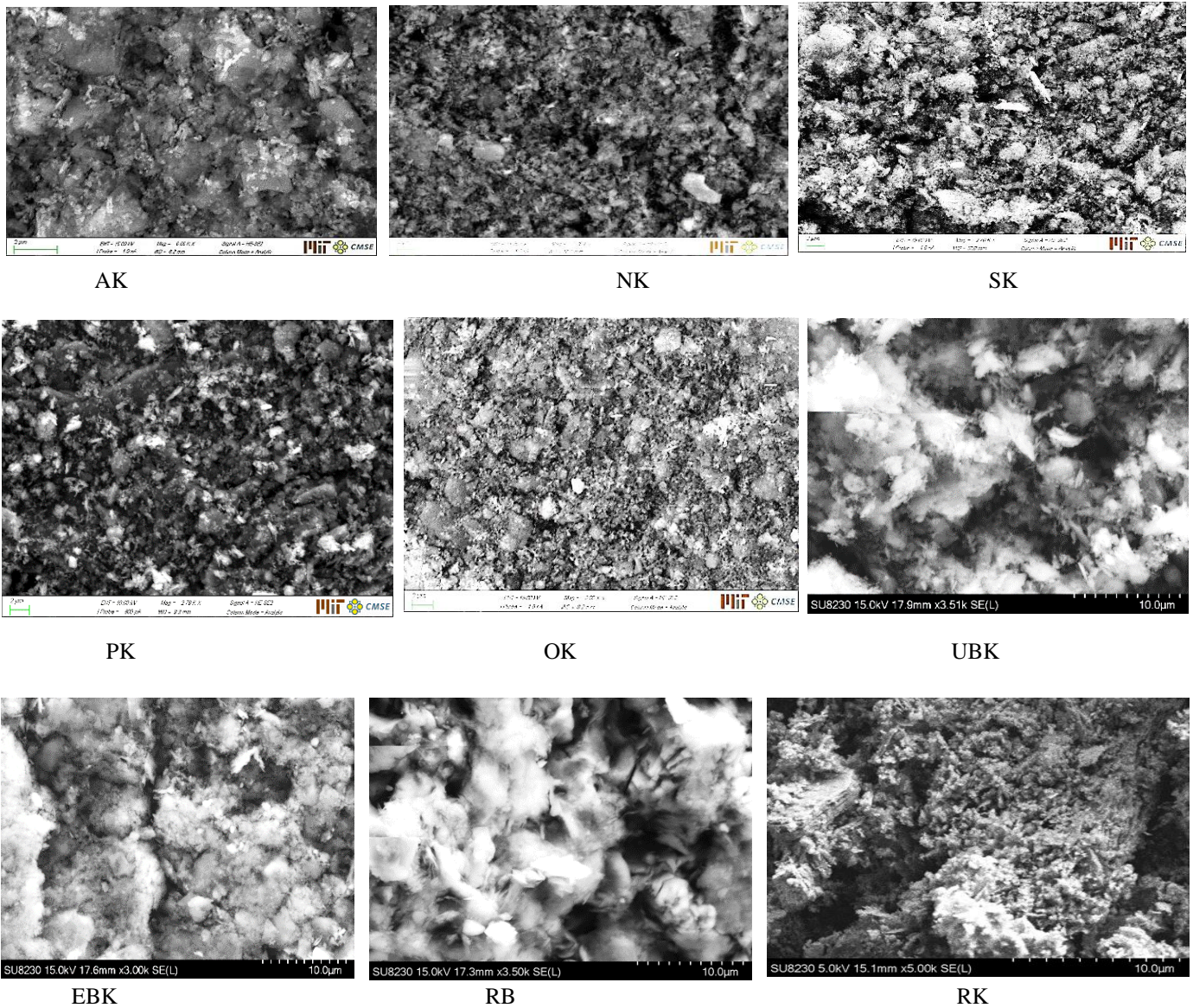


Figure 2: Scanning Electron Micrograph images of Raw kaolinite, AK, NK, SK, PK, OK, UBK, EBK, RB and RK

bands at 462.92, 682.80, and 532.35 cm^{-1} indicate bending vibrations of Si – O – Si and Si – Al – O and groups (Novakovic *et al.*, 2008), Bertagnolli and da Silva (2012) and Ozdes *et al.*, 2011).

The spectra in Figure 3b shows no appreciable changes in the absorption bands of the clay after acid treatment. However, further careful study of the FTIR raw data indicated that absorption bands at 3687.90, 3622.32 and 3618.46 cm^{-1} attributed to –OH stretching vibrations were retained only in acid activated clays SK, OK and PK but at reduced intensities. However, there was shift of the absorption band at 3687.90 cm^{-1} to 3689.83 cm^{-1} and 3684.04 cm^{-1} in NK and AK respectively. The absorption band at 1114.86 cm^{-1} was retained in most of the acid clays with lowered intensities except for NK where the intensity was higher. The absorption band at 1026.13 cm^{-1} shifted to 1028.06 cm^{-1} in NK while that at 1006.84 cm^{-1} shifted 1002.98 cm^{-1} in SK, OK and PK. The trio S-K, P-K and O-K exhibited shifts of the Al – Al – OH stretching vibrations at 914.26 cm^{-1} to 910.40 cm^{-1} and to 912.33 cm^{-1} in NK. There was a reduction in intensity of the absorption band at 790.81 cm^{-1} that was retained in all the acid activated samples except in NK where there was a shifted 788.89 cm^{-1} . The band at 682.80 cm^{-1} was maintained but with higher intensity in NK and a shift to 678.94 cm^{-1} in AK, OK, PK and SK with reduced intensities. In PK, OK and SK, the absorption band 532.35 cm^{-1} moved to 528.50 cm^{-1} and 534.28 cm^{-1} in NK but remained in AK. The 462 cm^{-1} absorption band assigned to Si – O – Si remained intact after acid treatment in most of the acid activated samples except in NK where it shifted to 464.84 cm^{-1} . The changes in intensities of original bands identified in the raw clay and movements of some to new positions in the acid activated samples suggest the dealumination of the clay and leaching of replaceable cations which is expected after acid treatment. Similar findings have been reported (Novakovic *et al.*, 2008, Akpomie and Dawodu, 2016 and Ihekwebe *et al.*, 2020).

The characteristic bands 3691.75 cm^{-1} and 3610.45 cm^{-1} of the kaolinite mineral are visible on the spectral of the composites. However, the intensities of the absorption bands of the clay composites E-BK and U-BK in Figure 3c were lower than those exhibited by the minerals independently over the entire IR region and this has been previously reported (Madejova *et al.*, 2002). In addition, the intensities of the band at 3622.32 cm^{-1} were higher than those of 3687.90 cm^{-1} band in both U-BK and E-BK because of the contribution of the bentonite (Madejova *et al.*, 2002). All FTIR bands exhibited by the raw sample RK were retained in U-BK except for Si – O – Si vibration bands at 1026.13 cm^{-1} and 1006.84 cm^{-1} that shifted to 1010.70 cm^{-1} and 1002.98 cm^{-1} respectively. In E-BK, the smectitic character was more pronounced in the bands 1624 cm^{-1} , 910.40 cm^{-1} and 528.50 cm^{-1} that represent –OH bending, Al – Al – OH stretching and Si – O – Al bending vibrations in the parent smectite respectively. Smectites are not usually easily detectable in Kaolinite/Smectite mixtures except at high content which was probably why smectitic character were only detected in the composite with the highest content of montmorillonite (Madejova *et al.*, 2002).

4) BET analysis results

A fundamental justification for modification of clay minerals is the improvement of the surface properties through the enhancement of the adsorption area and void capacity; properties that have been reported to be closely proportional to the adsorption tendencies and capacities of clay minerals (Sarma *et al.*, 2016 and Dim *et al.*, 2021). The surface areas of the adsorbents obtained from BET analysis along with their pore volumes and sizes are listed in Table 1a and b.

As can be observed from Table 1a, acid-activated clays NK, SK as well as OK have higher surface areas than the raw while reduction occurred in AK and PK. The order of which is NK (162.227 m^2/g) > SK (151.335 m^2/g) > OK (115.837 m^2/g) > RK (114.946 m^2/g) > PK (113.872 m^2/g) > AK (112.865 m^2/g).

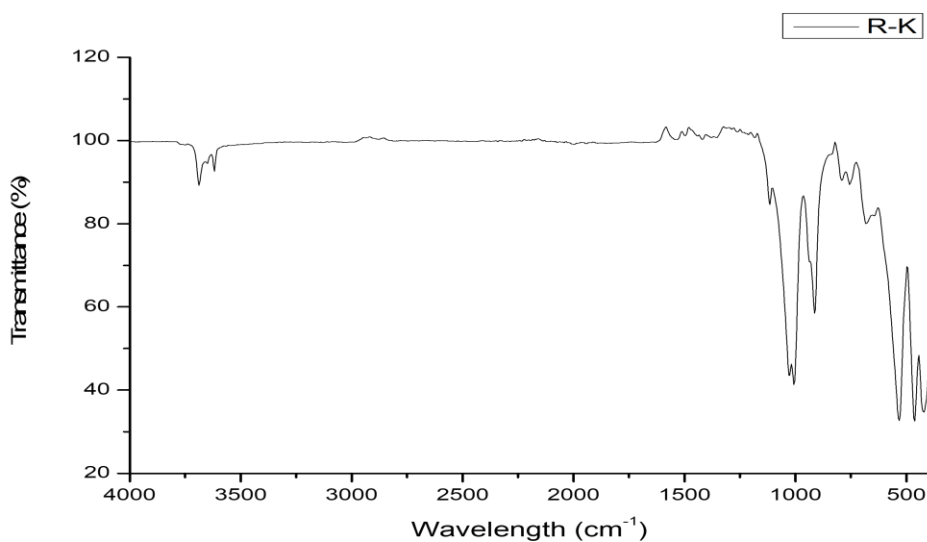


Figure 3a: FTIR spectrum of Raw Kaolinite (RK)

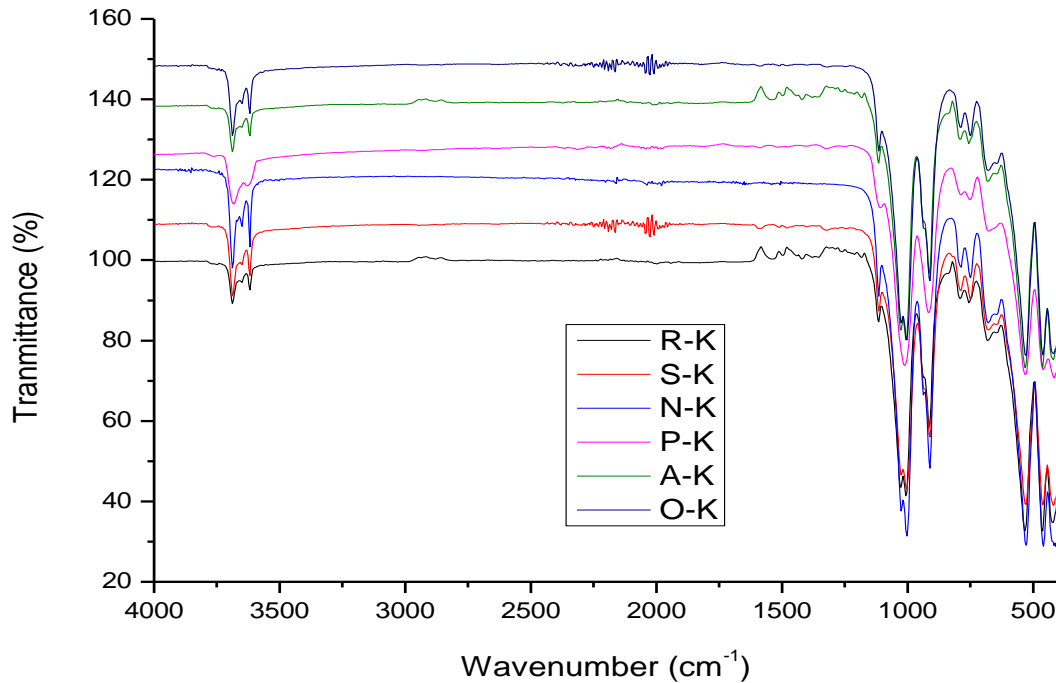


Figure 3b: Comparison of raw and acid-activated kaolinite clays spectra

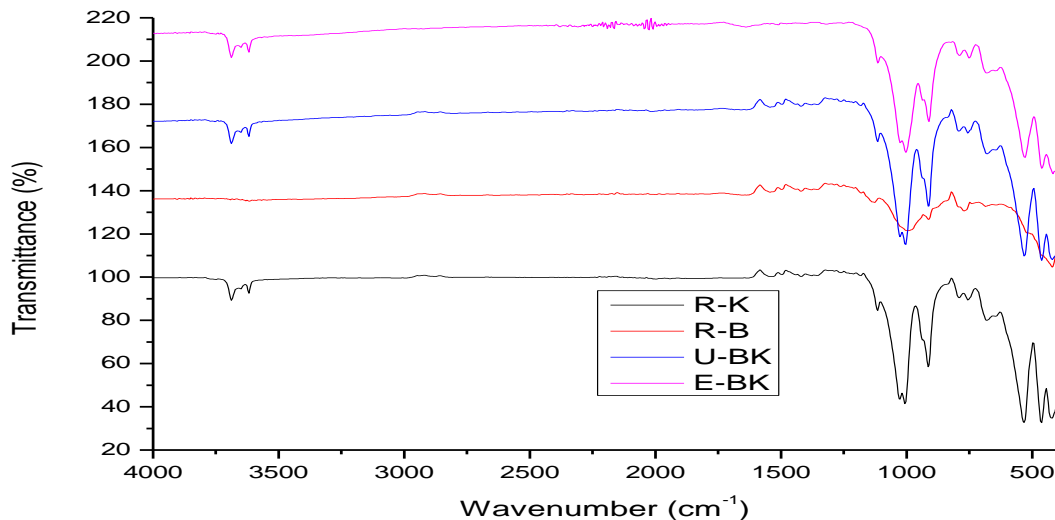


Figure 3c: Compared view of the raw and clay composites spectral

The increase was only substantial in strong acid clays NK and SK, moderately so for organic acid clay OK but lowered in the weakest acid clays AK and PK. There was a reduction in the total pore volume of AK ($0.51269 \text{ cm}^3/\text{g}$) from ($0.70588 \text{ cm}^3/\text{g}$) RK but increase in NK ($0.80587 \text{ cm}^3/\text{g}$), SK ($0.80055 \text{ cm}^3/\text{g}$), OK ($0.71187 \text{ cm}^3/\text{g}$) and PK ($0.71213 \text{ cm}^3/\text{g}$).

The acid-activated clays NK (11.84 nm), SK (16.03 nm) have lower pore diameters than RK (23.88 nm) which is less than those of OK (25.14 nm), PK (27.04 nm) and the highest AK (27.56 nm). These alterations in surface area, pore volume and size of the raw clay in the acid-activated clays can be attributed to removal of impurities, replacement of

exchangeable cations and generation of Silica. All these allowed more surface creation in most of the acid-activated forms. Reports of the enhancement of surface areas of clay minerals through acid activation have been documented in literature (Kumar *et al*, 2013, Alvarez, *et al* 2017, Dim *et al*, 2021 and Malima *et al*, 2021).

The surface areas of the composite (UBK ($205.92 \text{ m}^2/\text{g}$) and EBK ($288.685 \text{ m}^2/\text{g}$)) are both higher than that of the raw kaolinite (RK ($114.946 \text{ m}^2/\text{g}$)) but lower than the natural bentonite's (RB ($288.868 \text{ m}^2/\text{g}$)) as can be observed from Table 1b. The pore volume also increased and decreased in the composites as compared with the raw kaolinite and bentonite

respectively. The pore sizes however are lower in the composites than in the kaolinite but higher than that of the bentonite. This suggests that the introduction of bentonite into kaolinite mineral can increase its surface area (UBK) almost to the magnitude of the raw bentonite (EBK) depending on the amounts of each mineral in the composite. It is also noteworthy that the surface areas of the composites were also higher than those of the acid-activated clays, thus, the surface characteristics of kaolinite can be improved by preparing composites with bentonite mineral.

These findings correlate with earlier reports of effective adsorption of metal ions at higher pH values where less competition for adsorption sites between $[H_3O^+]$ and the positively ions is obtainable (Ozdes *et al.*, 2011, Sari and Tuzen, 2014, and Mohamed *et al.*, 2019). However, the investigation was not extended beyond pH 7 and 4.5 for Ni^{2+} as well as Cd^{2+} and Pb^{2+} respectively because precipitations of the metals were observed beyond these values especially for Pb^{2+} ions whose precipitation have been reported to occur from pH 5 (Lawal *et al.*, 2020) while other metals have also been

Table 1a: BET analysis result of raw and acid-Kaolinite

Parameter	RK	AK	NK	OK	PK	SK
BET surface area, S_{BET} (m ² /g)	114.946	112.865	162.227	115.837	113.872	151.335
Langmuir surface area (m ² /g)	260.374	194.491	274.091	268.049	256.956	267.503
External specific area (m ² /g)	123.275	80.5647	141.733	115.442	112.252	132.453
Micropore area (m ² /g)	19.3005	15.452	20.4937	19.169	20.3941	20.2247
Micropore volume (cm ³ /g)	0.00541	0.00617	0.00864	0.00626	0.00635	0.00706
Total pore volume (cm ³ /g)	0.70588	0.51269	0.80587	0.71187	0.71213	0.80055
Pore diameter (nm)	23.88	27.56	11.84	25.14	27.04	16.03

Table 1b: BET Analysis Results of raw and clay composites

Parameter	RK	RB	UBK	EBK
BET surface area, S_{BET} (m ² /g)	114.946	288.868	205.92	288.685
Langmuir surface area (m ² /g)	260.374	729.109	283.615	686.344
External specific area (m ² /g)	123.275	280.549	280.574	291.659
Micropore area (m ² /g)	19.3005	51.3943	25.128	22.8972
Micropore volume (cm ³ /g)	0.00541	0.02365	0.0083	0.0071
Total pore volume, (cm ³ /g)	0.70588	0.90848	0.72492	0.74956
Pore diameter (nm)	23.88	11.20	19.35	18.12

found to occur at higher pH values (Rahmani *et al.*, 2010, Dawodu and Akpomie, 2014, El-Naggar *et al.*, 2019). There have been reports where adsorption of the studied metals increased with increasing pH (Barka *et al.*, 2013, Akpomie and Dawodu, 2014, Krika *et al.*, 2016, El-Naggar *et al.*, 2018, Chai *et al.*, 2020).

B. Adsorption studies

1) Effect of pH

It is highly crucial to investigate the pH dependence of adsorption processes because the pH significantly influences the speciation and degree of ionization of the adsorbate ions as well as the surface charges of adsorbents (Rahmani *et al.*, 2010). In this study, the uptake of the heavy metal ions was found to be enhanced with increase in pH to a maximum of pH 7 for Cd^{2+} as well as Ni^{2+} and pH 4 for Pb^{2+} as shown in Figure 4a.

2) Effect of initial concentration

The optimum pH values (pH 4 for lead and pH 7 for Ni and Cd) obtained from the previous experiments were used for the determination of the effects of the initial concentrations of the heavy metal ions. All other condition were the same as the previous experiments except the concentrations of the metal solutions that were varied between 10-250 mg/L.

As represented by Figure 4b, the quantities of heavy metal ions removed increased with increase in their initial concentrations, and this can be attributed to increased concentration gradient obtainable at higher concentrations that created efficient mass exchange between the solid and liquid

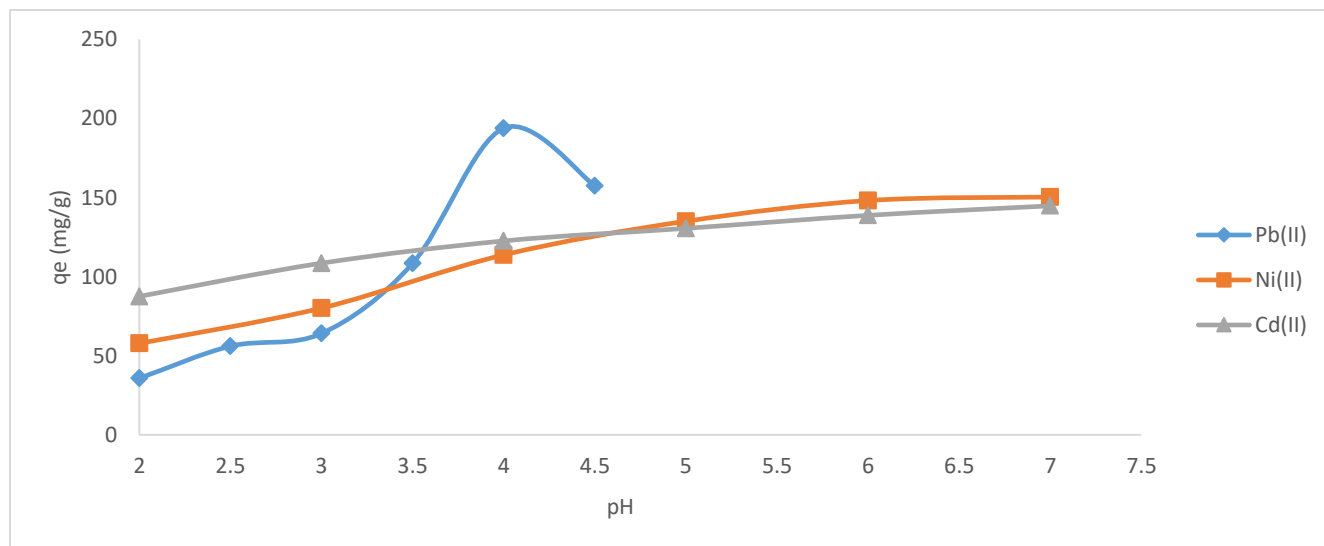


Figure 4a Influence of pH on the adsorption of heavy metal ions

phases (Akpomie and Dawodu, 2014, Mohamed *et al*, 2019).

However, this was obtainable to a maximum of 150 mg/L for Cd^{2+} and Ni^{2+} and 200 mg/L for Pb^{2+} because no significant change occurred in their removals after these concentrations probably as due saturation of the adsorbent's active sites at higher adsorbate that could have prevented continued deposition of metal ions on the adsorbent. Related findings have been reported by Ozdes *et al*, 2011, Ghogomu *et al*, 2013, Mhamdi *et al*, 2014 and Khalifa *et al*, 2020.

The overall assessment shows that the raw kaolinite mineral performed moderately in the adsorption of the studied heavy metal ions with 57% of Cd^{2+} , 60% of Ni^{2+} and 65% of Pb^{2+} , adsorbed in the order was $\text{Cd}^{2+} < \text{Ni}^{2+} < \text{Pb}^{2+}$. The adsorption of heavy metals has been reported to proceed through two different phenomena: complexation and ion exchange. If complexation is the primary mechanism, several factors come into focus such as the properties of the metals, functional groups present on the adsorbent, and pH of the solution (Chao and Chang, 2012, Saxena *et al*, 2017).

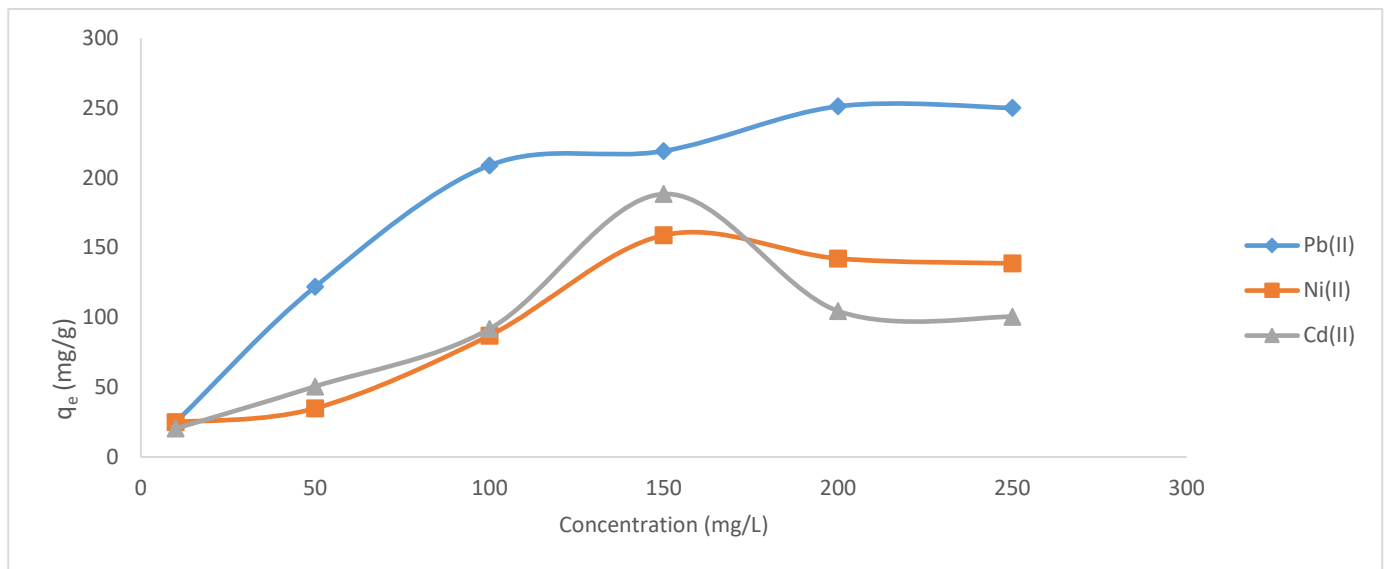


Figure 4b: Influence of initial concentration on the adsorption of heavy metal ions on Kaolinite

3) Effect of temperature

The optimum conditions (pH and initial concentration) determined from the previous experiments were used while the temperature was varied between 303-333 K, and all other factors were kept constant. The uptake of Pb^{2+} ions as can be seen from Figure 4c reduced with increasing temperature suggesting that some heat was evolved in the attachment of the ions to the adsorbent surface thus implying an exothermic process. On the other hand, initial increases and subsequent falls in adsorption were observed for both Cd^{2+} and Ni^{2+} ions with the least uptake of Cd^{2+} at the lowest temperature suggesting an endothermic process of adsorption of its ions. Similar findings have earlier been reported (Rahmani *et al*, 2010 and Resmi *et al*, 2011).

4) Effect of time

These investigations were conducted at 8 different time intervals between 10 mins-3.5 hrs utilizing optimum conditions determined from previous experiments. It was found that the highest removals of the heavy metal ions occurred at the initial time followed by progressive reductions in adsorption till the end of the period investigated for all three metals (Figure 4d). This is because of the high number of empty sites that were available for adsorption at initiation which reduces when most sites are filled as the period of contact becomes longer. This has also been previously reported (Omidi-Khaniabadi *et al*, 2017, Mohammed *et al*, 2019).

Conversely, if ion exchange was the case, the uptake of the investigated heavy metal ions would vary directly with the ionic radii, the increasing order of which is: $\text{Ni} < \text{Cd} < \text{Pb}$ (Chao and Chang, 2012). The metal ion with the highest potential to form complexes out of all three metals is Ni^{2+} while Pb^{2+} and Cd^{2+} accomplish relatively higher adsorption tendencies through the ion exchange. The order discovered in this study indicates that the adsorption process was a combination of both pathways. Another factor worth considering is the hydrated radii of the ions ($\text{Cd}^{2+} = 0.426$ nm, $\text{Ni}^{2+} = 0.404$ nm and $\text{Pb}^{2+} = 0.401$ nm), and hydration energy ($\text{Ni}^{2+} = -2106$ kJ mol⁻¹, $\text{Cd}^{2+} = -1807$ kJ mol⁻¹, $\text{Pb}^{2+} = -1481$ kJ mol⁻¹) (Mobasherpour *et al*, 2012 and Fan *et al*, 2021).

C. Isotherm modelling for adsorption of heavy metals on RK

The results obtained from the study of effect of initial concentration at equilibrium time were used for isotherm modelling using four models Fowler-Guggenheim, Langmuir, Freundlich, and Dubinin Radushkevich (DBR) equations as shown in Figures 5a-c while the obtained parameters are presented in Table 2.

It can be noted from Table 2 that the Langmuir isotherm gave the best fit for all the three heavy metals with the highest correlation coefficients of 0.9992, 0.9962 and 0.9927 for Cd^{2+} , Ni^{2+} , and Pb^{2+} respectively. The maximum adsorption capacities for the heavy metals were determined to be 109.89 mg g⁻¹, 126.58 mg g⁻¹ and 263.16 mg g⁻¹ for Cd^{2+} , Ni^{2+} , and

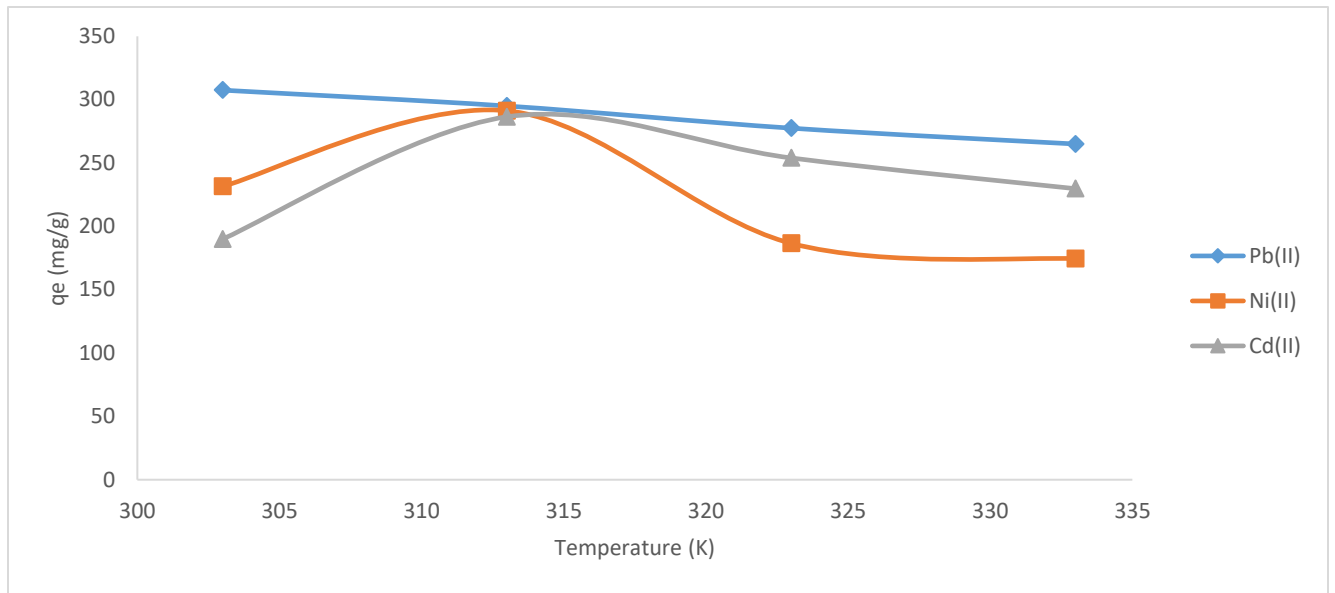


Figure 4c: Influence of temperature on the adsorption of heavy metal ions on Kaolinite

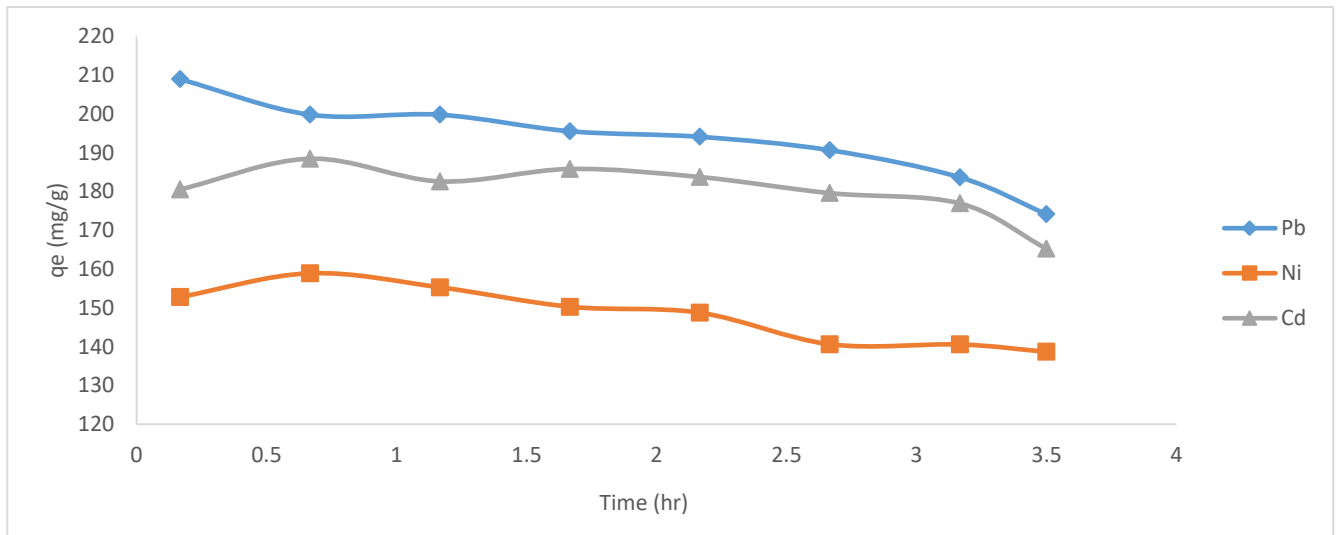


Figure 4d: Influence of time on the adsorption of heavy metal ions on Kaolinite

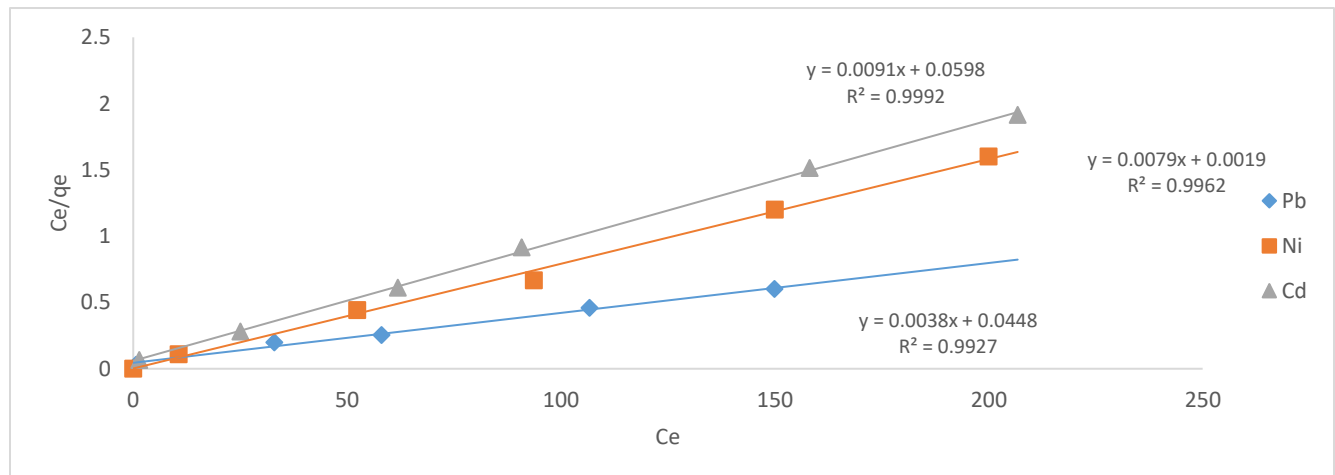


Figure 5a: Langmuir plots for the adsorption of heavy metal ions on RK

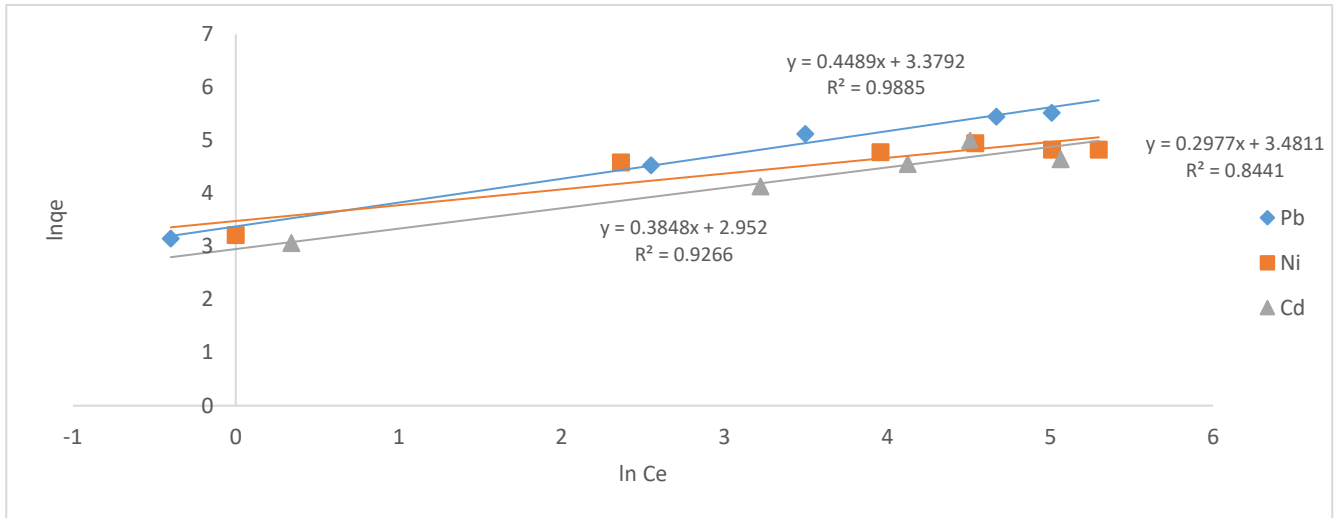


Figure 5b: Freundlich plots for the adsorption of heavy metal ions on RK

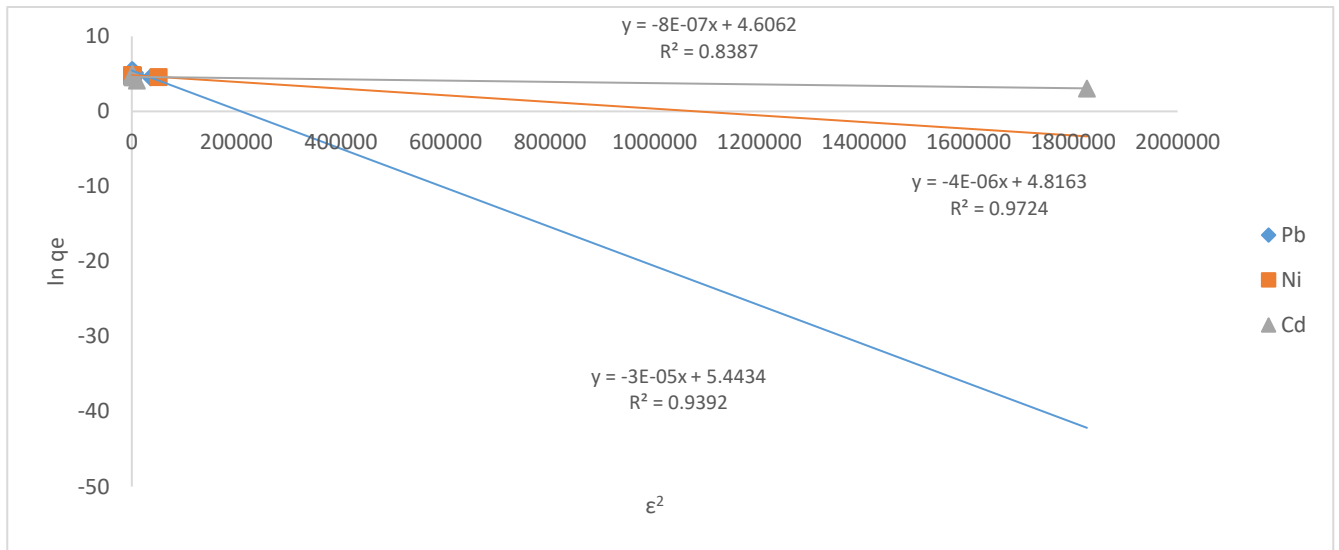


Figure 5c: Dubinin Radushkevich plots for the adsorption of heavy metal ions on RK

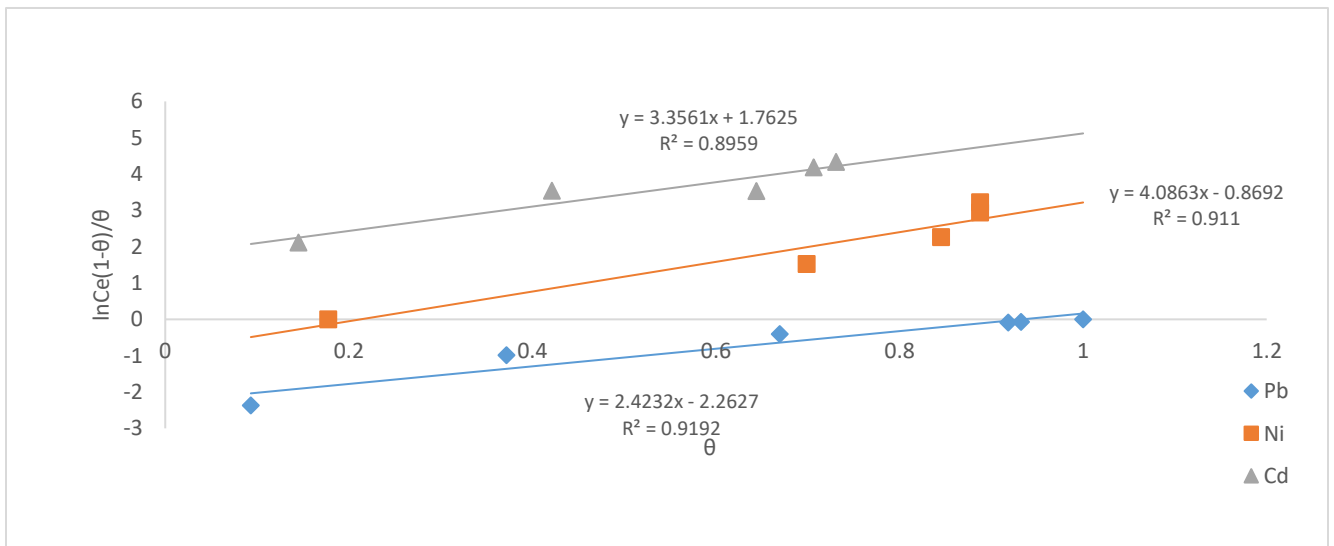


Figure 5d: Fowler-Guggenheim plots for adsorption of heavy metal ions on RK

Table 2 Parameters obtained from isotherm modelling

Isotherm models	Pb ²⁺	Ni ²⁺	Cd ²⁺
Langmuir model			
q _L (mg g ⁻¹)	263.16	126.58	109.89
K _L (L mg ⁻¹)	0.085	4.158	0.152
R ²	0.9927	0.9962	0.9992
Freundlich model			
K _F (mg g)(mg/L) ^{1/n}	29.35	32.50	19.14
n	2.23	3.36	2.60
R ²	0.9885	0.8441	0.9266
DBR model			
q _m (mg/g)	231.23	123.51	100.103
β (mol ²)(kJ ²) ⁵	3.0 E-	4.0E-5	8.0E-7
E (kJ/mol)	0.12	0.35	0.79
R ²	0.9392	0.9724	0.8387
FG model			
KFG (Lmg ⁻¹)	9.61	2.39	0.17
w (kJmol ⁻¹)	3.05	5.15	4.23
R ²	0.9192	0.911	0.8959

Pb²⁺ respectively indicating high adsorption capacity of the clay for the metals. Similar findings have been reported previously (Sari and Tuzen, 2014, Hai *et al.*, 2015, Yin *et al.*, 2018, Kakaei *et al.*, 2020).

The dimensionless Langmuir parameter of the equilibrium or adsorption intensity R_L was further calculated from the Langmuir equation at the different initial concentrations (C₀) investigated in the study and the values are presented in Table 3. There implications of R_L values are favourable adsorption (1 > R_L > 0), un-favorable adsorption 1 < R_L, linear adsorption R_L = 1 and R_L = 0 for irreversible adsorption (Ozdes *et al.* 2011, Gebretsadik *et al.*, 2020). From the values presented in Table 3. R_L values obtained for all the metals (0.045 - 0.541) for Pb, (0.001-0.023) for Ni and (0.026-0.397) for Cd suggest that their adsorption on the surface of the clay were favourable (Qin *et al.*, 2020, Malima *et al.*, 2021).

Table 3: Dimensionless R_L values at different initial concentrations of the three heavy metals

C ₀	R _L (Pb)	R _L (Ni)	R _L (Cd)
10	0.541	0.023	0.397
50	0.191	0.005	0.116
100	0.105	0.002	0.062
150	0.073	0.002	0.042
200	0.056	0.001	0.032
250	0.045	0.001	0.026

The regression coefficients obtained from the Freundlich isotherm were also considerable especially for Pb (0.9885) and Cd (0.9266). The K_F and n parameters of the isotherm give insight into the adsorption capacity as well as intensity of the adsorption respectively. For favourable adsorption, n values must fall within 1-10 (Chand and Pakade, 2015, Omer *et al.* 2018). The n values from the Freundlich isotherm fall within range that suggests favourable adsorption. In addition, the n values obtained for the three metal ions are all greater than one and these implies the physical nature of the adsorption process (Dada *et al.*, 2021, Nandiyanto, 2020).

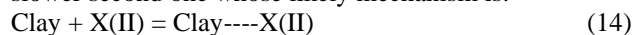
The E values obtained from the DBR equation were all lower than 8 kJ/mol which suggests that the adsorption of the metal ions was physical in nature and mostly through ion exchange mechanism (Inglezakis and Zorpas, 2011, Hu and Zhang, 2019). The positive w values obtained for the three metals from the FG equation suggest lateral interactions between adsorbed moles which indicate exothermic processes of adsorption. While this assumption correlates with the result obtained from the study of effect of temperature on the adsorption of metal ions Pb²⁺ and Ni²⁺, it is contradictory for Cd²⁺ as an endothermic process was found to be the case for the latter. This is probably due to low correlation co-efficient of its data to the isotherm compared to the other two (Hamdoui and Nefrecoux, 2007, Nandiyanto, 2020).

D. Kinetics of adsorption of heavy metals on R-K

The adsorption data was fitted into three different kinetic models viz pseudo-first order, pseudo-second order and Elovich models as shown in Figures 6a-c. It is apparent from these figures (6a-c) that the pseudo-second order gave the best fit for all the metals. The values of the obtained parameters are presented in Table 4.

The R² values obtained from the pseudo second order model [0.9628 (Cd), 0.9721 (Ni) and 0.9942 (Pb²⁺)] make it to be the best fit to the data. In addition, the derived q_e values (147.06 mg g⁻¹, 169.50 mg g⁻¹ and 238.10 mg g⁻¹ for Cd²⁺, Ni²⁺ and Pb²⁺ respectively) from the model are in good agreements with q_{exp} (155.31 mg g⁻¹, 179.58 mg g⁻¹ and 250.00 mg g⁻¹ for Cd²⁺, Ni²⁺ and Pb²⁺ respectively) values obtained from the experiments.

The major underlying principle of the pseudo-second-order model is that two reactions are occurring simultaneously: a fast reaction that attains equilibrium rapidly and a much slower second one whose likely mechanism is:



For such reaction as above, the kinetics is greatly influenced by the concentration of X(II) ions in the solution and the number of adsorption sites on the clay surface (Meneguín *et al.*, 2017, Yin *et al.*, 2018, Chai *et al.*, 2020). Several studies have reported the adsorption of the studied metal ions to be best described by pseudo-second order kinetic model (Galindo *et al.*, 2013, Krika *et al.*, 2016, Maged *et al.*, 2020, Kakaei *et al.*, 2020).

E. Thermodynamics of adsorption of heavy metals on raw kaolinite mineral

The Vant Hoff's plots for the adsorption of the three heavy metal ions RK are shown in Figures 7a-c and the thermodynamic parameters obtained are listed in Table 5.

In Table 4, ΔG values are negative for all the heavy metals which suggest spontaneous adsorption processes at the investigated temperatures except for Ni²⁺ at 333K (Malima *et al.*, 2020). The positive value suggests the non-spontaneity of adsorption of Ni²⁺ions at this temperature (El-Naggar *et al.*, 2018). For Ni²⁺ and Pb²⁺ ions, there were rises in ΔG values form (-1.94 – 0.22 kJ mol⁻¹) and (-3.49 – 2.87 kJ mol⁻¹) respectively which indicates more affinity between the adsorbent surface and the metal ions at lower rather than elevated temperatures while the converse was the case for Cd²⁺

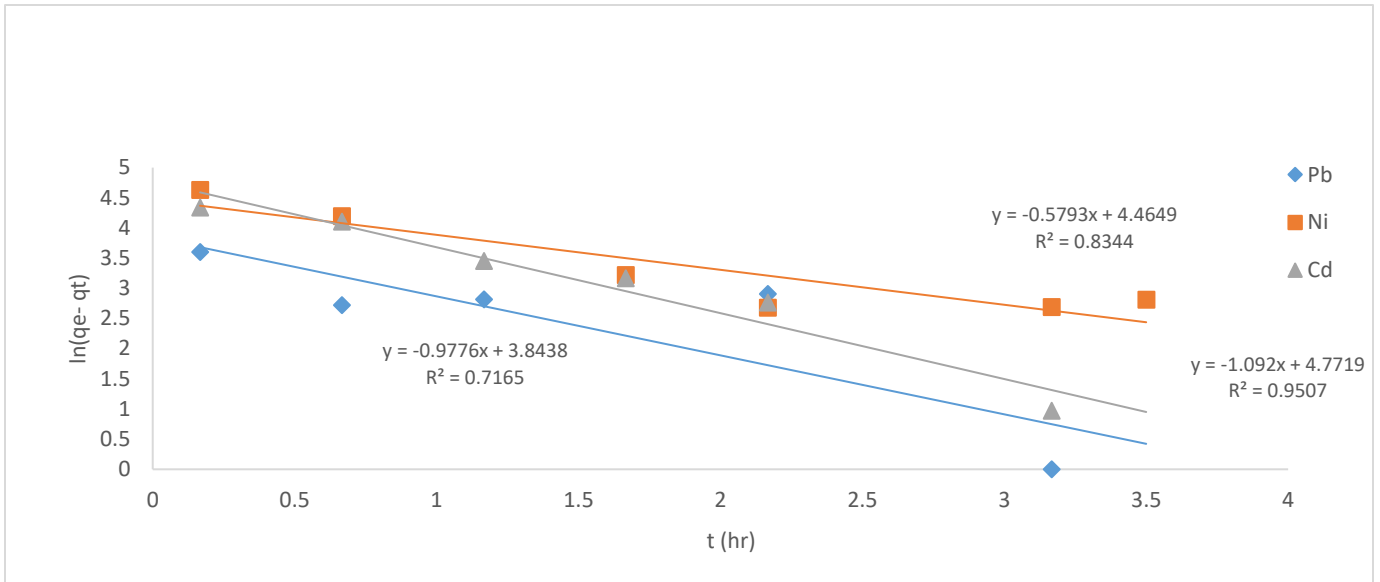


Figure 6a: Pseudo-first order plots for adsorption of heavy metal ions on RK

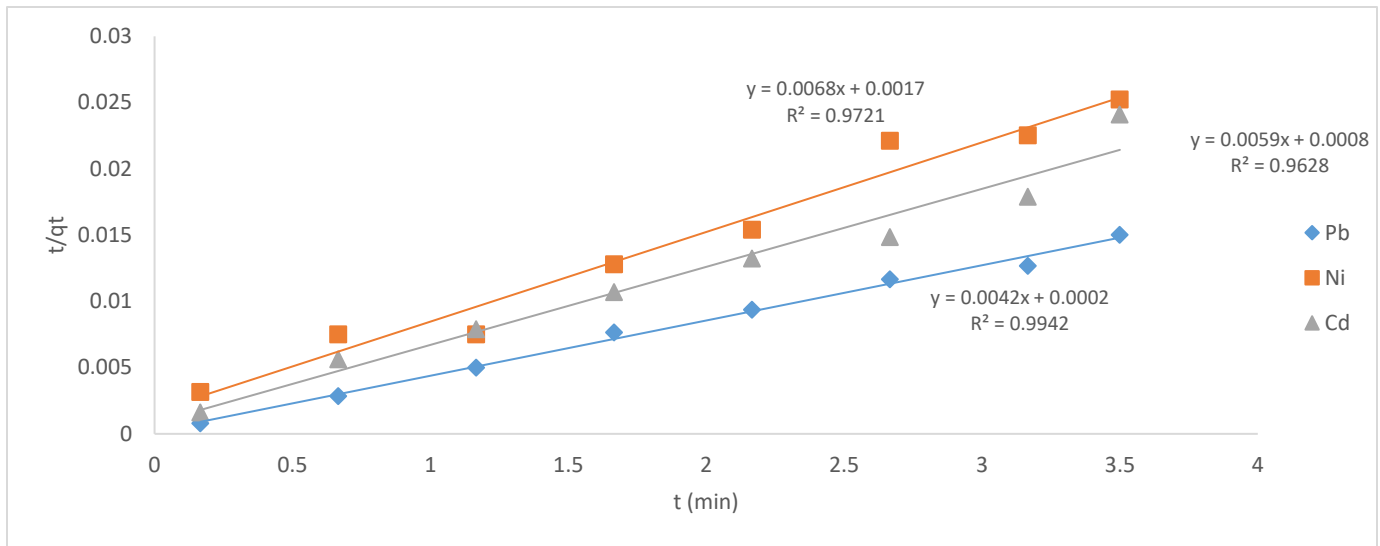


Figure 6b: Pseudo-second order plots for adsorption of heavy metal ions on RK

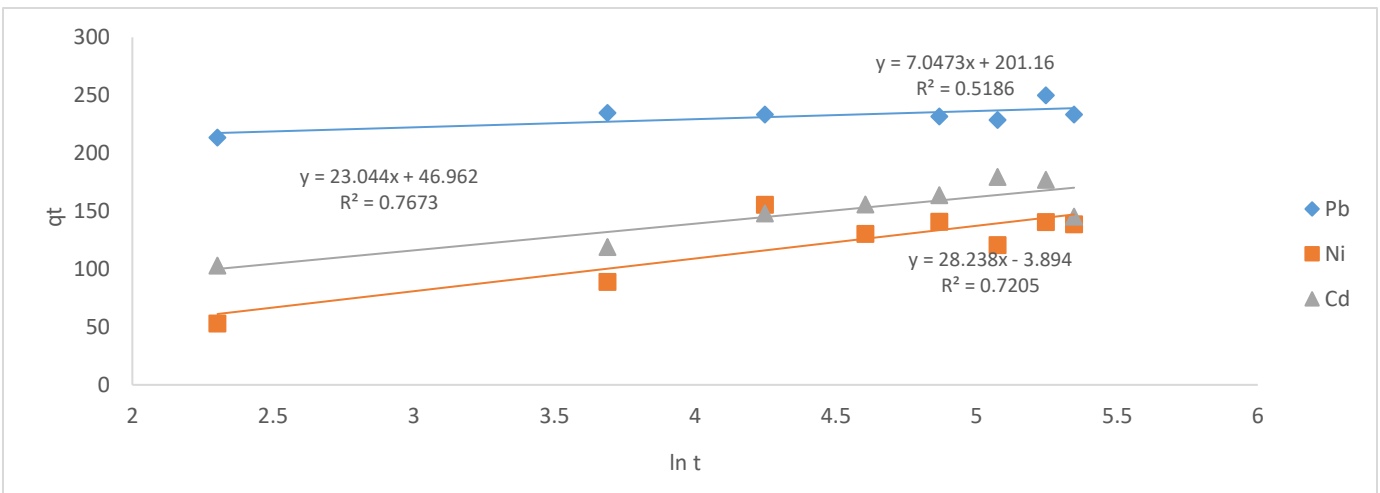


Figure 6c: Elovich plots for adsorption of heavy metal ions on RK

Table 4: Kinetic parameters of adsorption of heavy metal ions on RK

Kinetic models	Pb ²⁺	Ni ²⁺	Cd ²⁺
q _{exp} (mg g ⁻¹)	250.00	179.58	155.31
Pseudo-first order model			
q _{e cal} (mg g ⁻¹)	46.70	86.91	118.14
k ₁ (min ⁻¹)	0.9776	0.5793	1.092
R ²	0.7165	0.8344	0.9507
Pseudo-second order model			
q _{e cal} (mg g ⁻¹)	238.10	169.50	147.06
k ₂ (min ⁻¹)	0.0882	0.0272	0.004
R ²	0.9942	0.9721	0.9628
Elovich model			
α (mg g ⁻¹ min ⁻¹)	1.76E+13	24.60056	176.8555
β (g mg ⁻¹)	0.142	0.035413	0.043395
R ²	0.5186	0.7205	0.7673

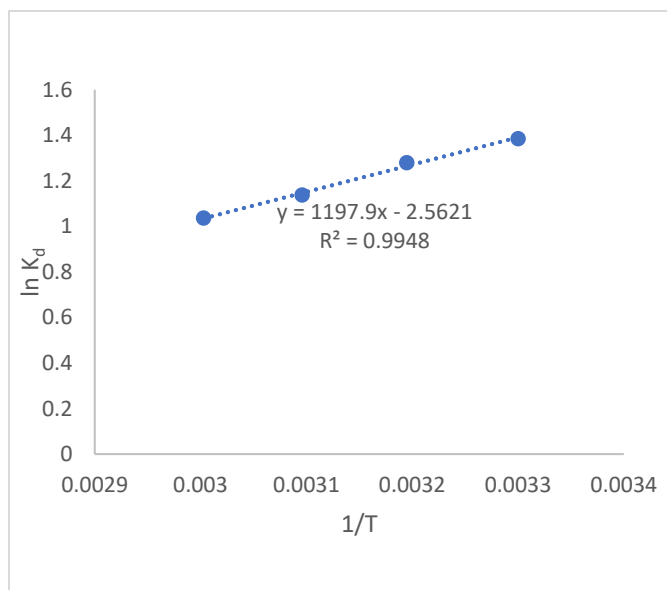


Figure 7a: Vant Hoff plot for the adsorption of Pb²⁺ ions on Kaolinite

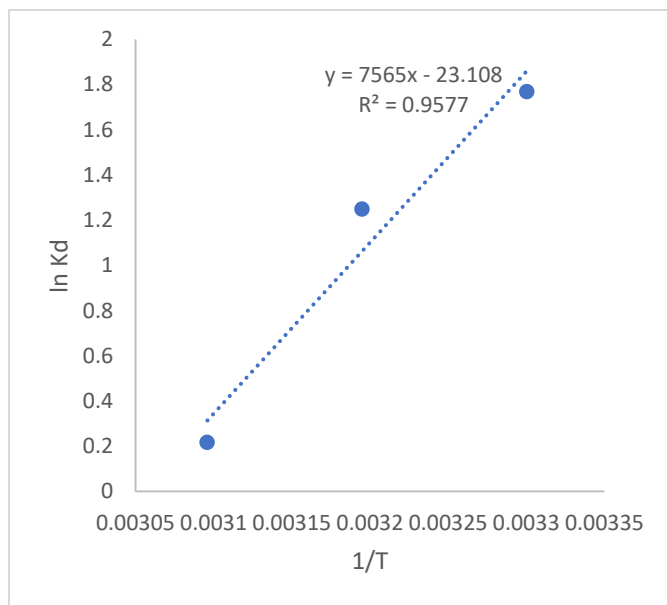


Figure 7b: Vant Hoff plot for the adsorption of Ni²⁺ ions on Kaolinite

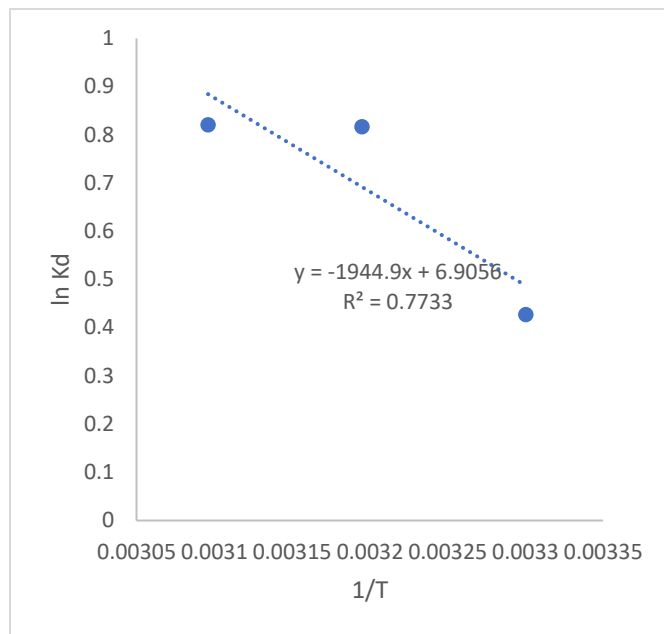


Figure 7c: Vant Hoff plot for the adsorption of Cd²⁺ ions on Kaolinite

Table 5: Thermodynamic parameters of adsorption of heavy metal ions on RK

Metal ion	ΔH (kJ mol ⁻¹)	ΔS (J mol ⁻¹)	ΔG (kJ mol ⁻¹)			
			303K	313K	323K	333K
Pb ²⁺	-9.96	-21.30	-3.49	-3.33	-3.05	-2.87
Ni ²⁺	-62.98	-192.12	-1.94	-3.25	-0.58	0.22
Cd ²⁺	16.17	57.41	-1.08	-2.12	-2.20	-2.01

ions whose ΔG values reduced from (-1.08 – -2.01 kJ mol⁻¹) (Eba *et al.*, 2013).

However, all the ΔG values obtained are lower than -5 kJ mol⁻¹ indicating physisorption process of adsorption (Mnasri-Ghnmimi and Srasra, 2019). The adsorption process was exothermic for Ni²⁺ and Pb²⁺ with ΔH values -9.96 kJ mol⁻¹ and -62.98 kJ mol⁻¹ respectively while being endothermic for Cd²⁺ with ΔH value 16.17 kJ mol⁻¹. The ΔS values were also negative for Ni²⁺ (-192.12 J mol⁻¹) and Pb²⁺ (-21.30 J mol) suggesting that there was lowering of randomness at the solid-liquid interface which could be a consequence of fixation of the metal ions on the surface of the adsorbent. Conversely, a positive value obtained for Cd²⁺ indicates increase in randomness at the interface and good affinity between the metal ion and the adsorbent surface (Akpomie and Dawodu, 2016, Rao and Khan, 2017).

F. Comparative adsorption of heavy metal ions on modified clays

The comparison of the performances of the modified clays in adsorbing the metal ions shown in Figure 8 revealed that the composites were more efficient than the raw and acid-activated kaolinite for the adsorption of the heavy metal ions from their respective aqueous solutions. The highest adsorption recorded on them was probably due to the presence of the bentonite that increased the number of exchangeable cations on the composites thus increasing the number of potential active sites for adsorption. As for the acid-activated

clays, the action of the acids on the clay would have occurred on and limited to the existing active sites on the clay. These results suggest that composite formation between Kaolinite and 2:1 clay can sufficiently enhance the adsorption tendencies of the former and provide a more environmentally friendly method of modifying the clay.

In addition, it can be observed from Figure 8b that the composites also performed better than the raw bentonite for Pb^{2+} and Cd^{2+} ions. These also confirm the advantage of manual composite formation between the two clay minerals because the clayey content of the bentonite was increased and thus enhanced its performance compared to the raw form.

V. CONCLUSION

The adsorption characteristics of a Nigerian Kaolinite in its raw and modified forms have been successfully evaluated. Acid modified kaolinites were prepared using inorganic and organic acids while clay composites were prepared by manually blending raw Kaolinite with a bentonite clay. Analytical techniques used for characterization confirmed the clays to be 1:1 (kaolinite) and 2:1 (Bentonite) minerals as well as the changes that occurred in their properties after modification. The BET surface area of the Kaolinite was significantly increased in the strong acid modified clays and the composites. Adsorption studies of three heavy metal ions

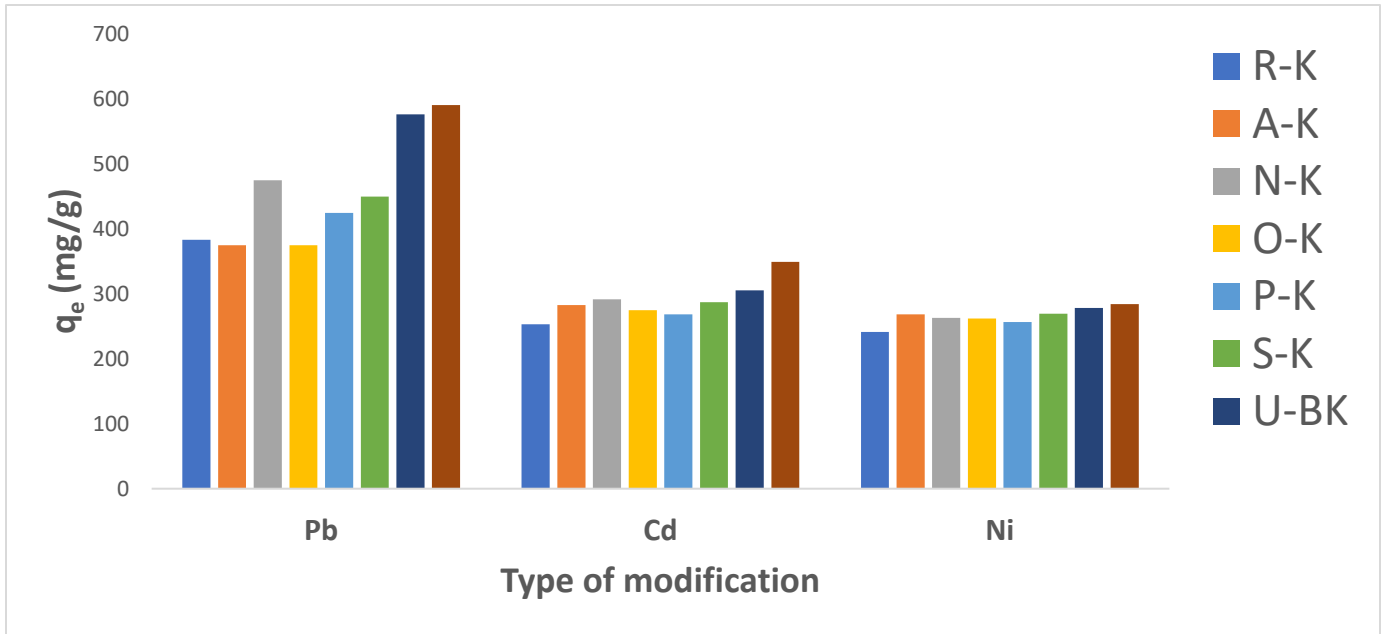


Figure 8a: Comparison of the adsorption efficiencies of the modified kaolinite clays

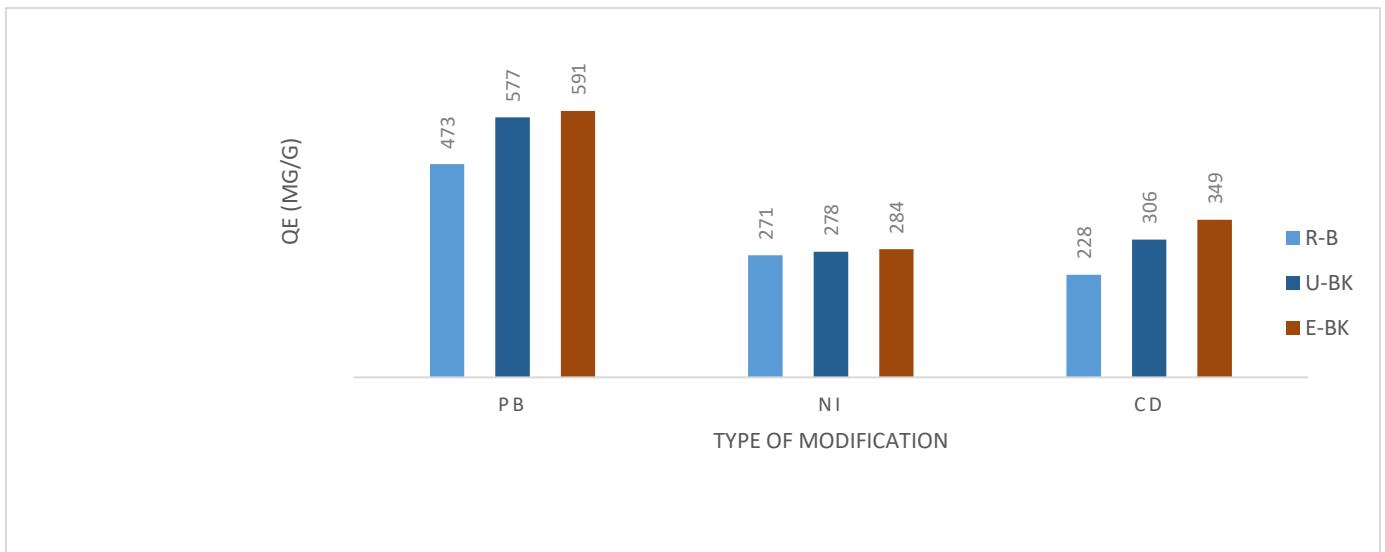


Figure 8b: Comparison of the adsorption efficiencies of the composites with the raw bentonite

were carried out on the raw clay minerals to determine optimum operating conditions of pH, time, initial metal concentration and temperature and time for each metal.

The determined conditions were used for investigations on the modified clays. The Langmuir isotherm was found to give the best correlation to the adsorption for the three heavy metal ions while the Pseudo second order model was the best for the kinetics. The Kaolinite was found to be moderate in adsorbing the heavy metal ions in its raw form, but the performance was highly enhanced through modification especially composite formation with a 2:1 mineral. Furthermore, acid activation with dilute acids enhanced the adsorption potentials of the kaolinite clay and for optimum results, dilute strong inorganic acids are recommended but weaker acids as well as organic acids can also be utilized. These results not only confirm the viability of clay minerals as suitable adsorbents for remediation of heavy metals polluted waters but also suggests that composite formation between Kaolinite and a 2:1 clay can sufficiently enhance the adsorption tendencies of the former thus providing a more environmentally friendly method of modifying the clay.

AUTHOR CONTRIBUTIONS

T. O. Abu: Conceptualization, Methodology, Validation, Writing – original draft, Writing – review & editing. **H. I. Adegoke:** Supervision, Methodology, Writing – review & editing. **E. O. Odebunmi:** Writing – review & editing. **M. A. Shehzad:** Methodology, Characterization, Writing – review & editing

REFERENCES

- Abechi, E.; C. Gimba; A. Uzairu and J. Kagbu. (2011).** Kinetics of adsorption of methylene blue onto activated carbon prepared from palm kernel shell. *Archives of Applied Science Research*, 3(1), 154-164.
- Adebowale, K.O.; E.I. Unuabonah and B.I. Olu-Owola. (2008).** Kinetics and Thermodynamic aspects of the adsorption of Pb^{2+} and Cd^{2+} ions on tripolyphosphate-modified kaolinite clay. *Chemical Engineering Journal*, 136, 99-107.
- Adeniyi, F. I.; M. B. Ogundiran; T. Hemalatha and B. B. Hanumantrai. (2020)** Characterization of raw and thermally treated Nigerian kaolinite-containing clays using instrumental techniques. *SN Applied Sciences*, 2, (821), 1-14.
- Akpomie, K. G. and Dawodu, F. (2016).** Acid-modified montmorillonite for sorption of heavy metals from automobile effluent. *Beni - Suef University Journal of Basic and Applied Sciences*, 5, 1–12.
- Al-Anber, M. A. (2011).** Thermodynamics Approach in the Adsorption of Heavy Metals. In J. M. Piraján (Ed.), *Thermodynamics - Interaction Studies - Solids, Liquids and Gases*. Shanghai, China: In Tech. pp. 737-764.
- Aljlil S.A. and Fares D. A., (2014).** Adsorption of Cu and Ni on bentonite clay from wastewater. *Athens journal of sciences*, 1(1):21-30.
- Almeida-Naranjo, C. E.; V. H. Guerrero and C. A. Villamar-Ayala. (2023).** Emerging Contaminants and Their Removal from Aqueous Media Using Conventional/Non-Conventional Adsorbents: A Glance at the Relationship between Materials, Processes, and Technologies. *Water*, 15, (1626), 1-47.
- Alshameri, A.; H. Hea; H. Zhua; Y. Xic; R. Zhua; L. Maa and Q. Tao. (2018).** Adsorption of ammonium by different natural clay minerals: Characterization, kinetics and adsorption isotherms. *Applied clay Science*, 159,83-93.
- Alvarez Acevedo, N. I.; M. C. G. Rocha and L. C. Bertolino. (2017).** Mineralogical characterization of natural clays from Brazilian Southeast region for industrial applications. *Cerâmica*, 63, 253-262.
- Anyakora, C.; K. Nwaeze; O. Awodele; C. Nwadi; M. Arbabi and H. Coker. (2011).** Concentrations of heavy metals in some pharmaceutical effluents in Lagos, Nigeria. *Journal of Environmental Chemistry and Ecotoxicology*, III (2), 25-31.
- Aragaw, T. A. and Bogale, F. M. (2021).** Biomass-Based Adsorbents for Removal of Dyes From Wastewater: A Review. *Frontiers in Environmental Science*, 9, (764958), 1-24.
- Aziz, K. H. H.; F. S. Mustafa; K. M. Omer; S. Hama; R. F. Hamaraw and K. O. Rahman. (2023).** Heavy metal pollution in the aquatic environment: efficient and low-cost removal approaches to eliminate their toxicity: a review, *RSC Advances*, 13(26): 17595–17610.
- Badmus, B. S. and Olatinsu, O. (2009).** Geophysical evaluation and chemical analysis of kaolin clay deposit of Lakiri village, South-western Nigeria. *International Journal of Physical Sciences*, 4 (10), 592-606.
- Bahl, A.; B. S. Bahl and G. D. Tuli. (2012).** Essentials of physical chemistry, S. Chand, New Delhi, pp 303-860.
- Balali-Mood M.; K. Naseri; Z. Tahergorabi; M. R. Khazdair and M. Shhi. (2021).** Toxic Mechanisms of Five Heavy Metals: Mercury, Lead, Chromium, Cadmium, and Arsenic. *Frontiers in Pharmacology*, 12 (643972) 1-18.
- Barka, N.; M. Abdennouri; M. El Makhfouk and S. Qourzal. (2013).** Biosorption characteristics of cadmium and lead onto eco-friendly dried cactus (*Opuntia ficus indica*) cladodes. *Journal of Environmental Chemical Engineering*, 1, 144–149.
- Bennour, H. A. M. (2017).** Effect of Acid Activation on Adsorption of Iron and Manganese Using Libyan Bentonite Clay, *Chemical Science Transactions*, 6, (2), 209-218.
- Berihun, D. and Solomon, Y. (2017).** Assessment of the Physicochemical and Heavy Metal Concentration from Effluents of Paint Industry in Addis Ababa, Ethiopia. *International Journal of Waste Resources*, 7(4), 1-5.
- Bertagnolli, C. and Carlos da Silva, M. G. (2012).** Characterization of Brazilian Bentonite Organoclays as Sorbents of Petroleum-derived Fuels. *Materials Research*, 15, (2), 253-259.
- Bhattacharyya, K. G. and Gupta, S. S. (2008).** Adsorption of a few heavy metals on natural and modified kaolinite and montmorillonite: A review. *Advances in Colloid and Interface Science*, 140, 114–131.
- Boparai, H. K.; M. Joseph and D. O'Carroll. (2011).** Kinetics and thermodynamics of cadmium ion removal by adsorption onto nano zerovalent iron particles. *Journal of Hazardous Materials*, 186(1), 458-465.

- Bukalo, N. N.; G. E. Ekosse; J. O. Odiyo and J. S. Ogola. (2017).** Fourier Transform Infrared Spectroscopy of Clay Size Fraction of Cretaceous-Tertiary Kaolins in the Douala Sub-Basin, Cameroon. *Open Geosciences*, 9, 407–418.
- Chai, J. -B.; P. -I. Au; N. M. Mubarak; M. Khalid; W. P. -Q. Ng; P. Jagadish; R. Walvekar and E. C. Abdullah. (2020).** Adsorption of heavy metal from industrial wastewater onto low-cost Malaysian kaolin clay-based adsorbent. *Environmental Science and Pollution Research*, 27, (12), 13949 – 13962.
- Chand, P. and Pakade, Y. B. (2015).** Synthesis and characterization of hydroxyapatite nanoparticles impregnated on apple pomace to enhanced adsorption of Pb(II), Cd(II), and Ni(II) ions from aqueous solution, *Environmental Science and Pollution Research*, 22, (14), 10919-10929.
- Chao, H. -P., and Chang, C. -C. (2012).** Adsorption of copper (II), cadmium (II), nickel (II) and lead(II) from aqueous solution using biosorbents, *Adsorption*, 18, 395–401.
- Chen, H. and Zhao, J. (2009).** Adsorption study for removal of Congo red anionic dye using organo-attapulgite. *Adsorption*, 15, 381–389.
- Crini, G.; E. Lichtfouse; L. Wilson and N. Morin-Crini. (2019).** Conventional and non-conventional adsorbents for wastewater treatment. *Environmental Chemistry Letters*, 17, (1), 195-213.
- Dada, A. O.; F. A. Adekola; E. O. Odebunmi; A. S. Ogunlaja and O. S. Bello. (2021).** Two–three parameters isotherm modeling, kinetics with statistical validity, desorption, and thermodynamic studies of adsorption of Cu (II) ions onto zerovalent iron nanoparticles, *Scientific reports*, 11, (16454), 1-15.
- Daniel-Mkpume, C. C.; P. O. Offora and S. Obiorah. (2011).** Compositing of Nsu And Ibeku Clays: A Solution Towards The Replacement of GP 107-3 Refractory Brick In The Metallurgical Industry. *Nigerian Journal of Technology*, 3(2), 67-72.
- Dawodu, F. A. and Akpomie, K. G. (2014).** Simultaneous adsorption of Ni(II) and Mn(II) ions from aqueous solution unto a Nigerian kaolinite clay. *Journal of Materials Research and Technology*, 3(2), 129–141.
- Dim, P. E.; L. S. Mustapha; M. Termtanun and J. O. Okafor. (2021).** Adsorption of chromium (VI) and iron (III) ions onto acid-modified kaolinite: Isotherm, kinetics and thermodynamics studies, *Arabian Journal of Chemistry*, 14, (103064), 1-14.
- Do, D. D. (1998).** Adsorption Analysis: Equilibria and Kinetics; Series on Chemical Engineering, Vol. 2, Imperial College Press, London. pp 7-101.
- Eba, F.; J. Ndong Nlo; J. Ondo; P. Andeme Eyi and E. Nsi-Emvo. (2013)** Batch experiments on the removal of U(VI) ions in aqueous solutions by adsorption onto a natural clay surface, *Journal of Environment and Earth Science*, 3, (1), 11-23.
- Edoziuno, F. O.; F. I. Iloghalu; M. C. Akaeze; N. O. Umeohia; C. C. Nwaeju and F. A. Anene. (2016).** A study of casting characteristics of some Nigerian clay slips for industrial production. *International Journal of Advanced Scientific Research*, 1(2), 41-45.
- Elgamouz, A.; N. Tijani; I. Shehadi; K. Hasan and M. Kawam. (2019).** Characterization of the firing behaviour of an illite-kaolinite clay mineral and its potential use as membrane support, *Heliyon*, 5, e02281, 1-9.
- El-Naggar, I. M.; S. A. Ahmed; N. Shehata; E. S. Sheneshen; M. Fathy and A. Shehata. (2019).** A novel approach for the removal of lead (II) ion from wastewater using Kaolinite/Smectite natural composite adsorbent. *Applied Water Science*, 9, (7), 1-13.
- Emam A.A.; L.E.M. Ismail and M.A. Abdelkhalek. (2016).** Adsorption study of some heavy metal ions on modified kaolinite. *International journal of Advancement in Engineering Technology, Management and Applied Science*. 3(7):152-163.
- Es-said, A.; H. Nafai; G. Lamzougui; A. Bouhaouss and R. Bchitou. (2021).** Comparative adsorption studies of cadmium ions on phosphogypsum and natural clay, *Scientific African*, 13, (e00960), 1-10.
- Ewere, E. E.; M. O. Omoigberale; O. E. Bamawo and N. O. Erhunmwunse. (2014).** Physio-Chemical Analysis of Industrial Effluents in parts of Edo States Nigeria. *Journal of Applied Sciences and Environmental Management*, 18(2), 267-272.
- Fan, X.; H. Liu; E. Anang and D. Ren. (2021).** Effects of Electronegativity and Hydration Energy on the Selective Adsorption of Heavy Metal Ions by Synthetic NaX Zeolite. *Materials*, 4, (15), 4066.
- Foo, K. Y. and Hameed, B. H. (2010).** Insights in to the modeling of adsorption isotherm systems. *Chemical Engineering Journal*, 156, 2–10.
- Galindo, L. S. G.; A. F. Neto; M. G. C. da Silva and M. G. A. Vieira. (2013).** Removal of Cadmium (II) and Lead(II) Ions from Aqueous Phase on Sodic Bentonite, *Materials Research*, 16, (2), 515-527.
- Gaya U.I.; E. Otene and A.H. Abdullah. (2015).** Adsorption of aqueous Cd (II) and Pb (II) of activated carbon nanopores prepared by chemical activation of Doum palm shell. *Springer plus* 4:458.
- Gebresadik, H.; A. Gebrekidan and L. Demlie. (2020).** Removal of heavy metals from aqueous solutions using *Eucalyptus Camaldulensis*: An alternate lowcost adsorbent, *Cogent Chemistry*, 6, (1), 1-16.
- Ghogomu, J. N.; T. D. Noufame; M. J. Ketcha and N. J. Ndi. (2013).** Removal of Pb (II) Ions from Aqueous Solutions by Kaolinite and Metakaolinite Materials, *British Journal of Applied Science & Technology*, 3, (4), 942-961.
- Guerra, D. J. L.; J. Goco; J. Nascimento and I. Melo. (2016).** Adsorption of divalent metals on natural and functionalized nontronite hybrid surfaces: An evidence of the chelate effect. *Journal of Saudi Chemical Society*, 20, S552–S565.
- Gupta, V. K.; P. J. Carrott; M. M. Ribeiro Carrott and Suhas. (2009).** Low-Cost Adsorbents: Growing Approach to Wastewater Treatment—a Review. *Critical Reviews in Environmental Science and Technology*, 39, 783–842.
- Hai, Y.; X. Li; H. Wua; S. Zhao; W. Deligeer and S. Asuha. (2015).** Modification of acid-activated kaolinite with TiO₂ and its use for the removal of azo dyes, *Applied Clay Science*, 114, 558–567.

- Hamdaoui, O. and Naffrechoux, E. (2007).** Modeling of adsorption isotherms of phenol and. *Journal of Hazardous Materials* 147, 381–394.
- Hao, Y.-f.; L.-g. Yan; H.-q. Yu; K. Yang; S.-j. Yu; Shan R.-r. and Du, B. (2014).** Comparative study on adsorption of basic and acid dyes by hydroxy-aluminum pillared bentonite. *Journal of Molecular Liquids*, 199, 202–207.
- Ho, Y. S. and McKay, G. (1999).** Pseudo-second order model for sorption processes. *Process Biochemistry*, 34, 451–465.
- Ho, Y.; C. Chiang and Y. Hsu. (2001).** Sorption Kinetics for Dye Removal from Aqueous Solution Using Activated Clay. *Separation Science and Technology*, 36(11), 2473–2488.
- Hoosiar, A.; P. Uhlik; D. G. Ivey; Q. Liu and T. H. Etsell. (2012).** Clay minerals in nonaqueous extraction of bitumen from Alberta oil sands Part 2. Characterization of clay minerals, *Fuel Processing Technology*, 96, 183-194.
- Hu, Q., and Zhang, Z. (2019).** Application of Dubinin–Radushkevich isotherm model at the solid/solution interface: A theoretical analysis, *Journal of Molecular Liquids*, 277, 646–648.
- Huang, X.; H. Zhao; G. Zhang; J. Li; Y. Yang and P. Ji. (2020).** Potential of removing Cd(II) and Pb(II) from contaminated water using a newly modified fly ash, *Chemosphere* 242, (125148), 1-10.
- Ihekweze, G. O.; J. N. Shondo; K. I. Orisekeh; G. M. Kalu-Uka; I. C. Nwuzor and A. P. Onwualu. (2020).** Characterization of certain Nigerian clay minerals for water purification and other industrial applications, *Heliyon* ,6, e03783, 1-11.
- Inglezakis, V. J. and Zorpas, A. A. (2011).** Heat of adsorption, adsorption energy and activation energy in adsorption and ion exchange systems, *Desalination and Water Treatment*, 39, 149-157.
- James, O. O.; K. Nwaeze; E. Mesagan; Agbojo; M., Saka, K. L. and Olabanji, D. J. (2013).** Concentration of Heavy Metals in Five Pharmaceutical Effluents in Ogun State Nigeria. *Bulletin of Environment, Pharmacology and Life Sciences*, 2(8), 84-90.
- Kakaei, S.; E. S. Khameneh; M. H. Hosseini and M. M. Moharreri. (2020).** A modified ionic liquid clay to remove heavy metals from water: investigating its catalytic activity *International Journal of Environmental Science and Technology*, 17, 2043–2058.
- Khalfa, L.; A. Sdiri; M. Bagane and M. L. Cervera. (2020).** Multi-element modeling of heavy metals competitive removal from aqueous solution by raw and activated clay from the Aleg formation (Southern Tunisia). *International Journal of Environmental Science and Technology*, 17, 2123–2140.
- Krika, F.; N. Azzouz and M. C. Ncibi. (2016).** Adsorptive removal of cadmium from aqueous solution by cork biomass: Equilibrium, dynamic and thermodynamic studies. *Arabian Journal of Chemistry*, 9, (2), 1077-1083.
- Kumari, N. and Mohan, C. (2021).** Basics of Clay Minerals and Their Characteristic Properties. *Clay and Clay Minerals*. *IntechOpen*. Available at: <http://dx.doi.org/10.5772/intechopen.97672>. Retrieved on 27/12/2023.
- Kumar, A. and Lingfa, P. (2020).** Sodium bentonite and kaolin clays: Comparative study on their FT-IR, XRF, and XRD, *Materials Today: Proceedings*, 22, 737-742.
- Kumar, S.; A.K. Panda and R. K. Singh. (2013).** Preparation and Characterization of Acids and Alkali Treated Kaolin Clay. *Bulletin of Chemical Reaction Engineering & Catalysis*, 8 (1), 61 – 69.
- Lawal J.A.; E.O. Odeunmi and F.A. Adekola. (2020).** Adsorption of Fe²⁺, Pb²⁺, Zn²⁺ and Cr⁶⁺ ions from aqueous solutions using natural, ammonium oxalate and sodium hydroxide modified kaolinite clay. *Ife Journal of Science* 22(3): 001-023.
- Levine, I. N. (2009).** Physical chemistry, Mc-Graw hill international edition, Mc-Graw Hill, New York. pp 161-575.
- Likita, M. B.; G. K. Nura; C. D. Nuhu and S. D. Isah. (2016).** Physico-Chemical Characterization of Industrial Effluents in Minna Niger State, Nigeria. *International Journal of Modern Analytical and Separation Sciences*, 5(1), 12-19.
- Madejova, J.; J. Keckes; H. Palkova and P. Komadel. (2002).** Identification of components in smectite/kaolinite mixtures. *Clay Minerals*, 37, 377–388.
- Maged, A.; I. S. Ismael; S. Kharbish; B. Sarkar; S. Peräniemi and A. Bhatnagar. (2020).** Enhanced interlayer trapping of Pb (II) ions within kaolinite layers: intercalation, characterization, and sorption studies. *Environmental Science and Pollution Research* 27, 1870–1887.
- Malima, N. M.; S. J. Owonubi; E. H. Lugwisha and A. S. Mwakaboko. (2021).** Thermodynamic, isothermal, and kinetic studies of heavy metals adsorption by chemically modified Tanzanian Malangali kaolin clay, *International Journal of Environmental Science and Technology*, 18, (10), 3153-3168.
- Meneguín, J. G.; M. P. Moisés; T. Karchiyappana; S. H. B. Fariaa; M. L. Gimenes; M. S. D. de Barros and S. Venkatachalam. (2017).** Preparation and characterization of calcium treated bentonite clay and its application for the removal of lead and cadmium ions: Adsorption and thermodynamic modelling, *Process Safety and Environmental Protection*, 111, 244–252.
- Mhamdi, M.; E. Elaloui and M. Trabelsi-Ayadi. (2013).** Kinetics of cadmium adsorption by smectite of Oued Tfal (Gafsa Basin). *Desalination and Water Treatment*, 52, 4245–4256.
- Mnasri-Ghnimi, S. and Srasra, N. (2019).** Removal of heavy metals from aqueous solutions by adsorption using single and mixed pillared clays, *Applied Clay Science*, 179, (105151), 1-17.
- Mobasherpour, I.; E. Salahi and M. Pazouki. (2012).** Comparative of the removal of Pb²⁺, Cd²⁺ and Ni²⁺ by nano crystallite hydroxyapatite from aqueous solutions: Adsorption isotherm study, *Arabian Journal of Chemistry*, 5, 439-446.
- Mohamed, H. S.; N. K. Soliman; D. A. Abdelrheem; A. A. Ramadan; A. H. Elghandour and S. A. Ahmed. (2019).** Adsorption of Cd²⁺ and Cr³⁺ ions from aqueous solutions by using residue of *Padina gymnospora* waste as promising low-cost adsorbent. *Heliyon*, 5, e01287, 1-32.

- Mohammed-Azizi, F.; S. Dib and M. Boufatit. (2013).** Removal of heavy metals from aqueous solutions by Algerian bentonite. *Desalination and Water Treatment*, 51, 4447–4458.
- Moretti, L.; S. Natali; A. Tiberi and A. D'Andrea. (2020).** Proposal for a Methodology Based on XRD and SEM-EDS to Monitor Effects of Lime-Treatment on Clayey Soils, *Applied Sciences* 10, 2569, 1-17.
- Mukhopadhyaya, R.; K.M. Manjaiaha; S.C. Dattaa; R. K. Yadav and B. Sarkarc. (2017).** Inorganically modified clay minerals: Preparation, characterization, and arsenic adsorption in contaminated water and soil, *Applied clay Science*, 147, 1-10.
- Nandiyanto, A. B. D. (2020).** Isotherm Adsorption of Carbon Microparticles Prepared from Pumpkin (*Cucurbita maxima*) Seeds Using Two-Parameter Monolayer Adsorption Models and Equations, *Moroccan Journal of Chemistry*, 8, (3), 745-761.
- Nordin, N. A.; N. Abdul Rahman and A. Abdullah. (2020).** Effective Removal of Pb(II) Ions by Electrospun PAN/Sago Lignin-Based Activated Carbon Nanofibers, *Molecules*, 25, (3081), 1-21.
- Novakovic', T.; L. Rozi'c'; S. Petrovic' and A. Rosic'. (2008).** Synthesis and characterization of acid-activated Serbian smectite clays obtained by statistically designed experiments, *Chemical Engineering Journal*, 137, 436–442.
- Olaofe, O.; S.A. Olagboye; P.S. Akanji; E.Y. Adamolugbe; O.T. Fowowe and A.A. Olaniyi. (2015).** Kinetic studies of adsorption of heavy metals on clays. *International Journal of Chemistry*, 7(1), 48-54.
- Olise, F. S.; S. B. Ola and F. A. Balogun. (2018),** Characterisation of clay samples from minerals– rich deposits for thermoluminescence applications, *Journal of King Saud University-Science*, 30, 158-167.
- Olusola, J.O.; A.A. Suray; M.A. Temitope and O.A. Aminat. (2011).** Sedimentological and geochemical studies of Maastrichtian clays in Bida Basin, Nigeria: Implication for resource potential. *Centre Point Journal (Science Edition)*, 17(2), 71-88.
- Omer, O. S.; M. A. Hussein; B. H. Hussein and A. Mgaidi. (2018).** Adsorption thermodynamics of cationic dyes (methylene blue and crystal violet) to a natural clay mineral from aqueous solution between 293.15 and 323.15 K. *Arabian Journal of Chemistry*, 11, 615–623.
- Omidi Khaniabadi, Y.; H. Basiri; H. Nourmoradi; M. J. Mohammadi; A. R. Yari; S. Sadeghi and A. Amrane. (2017).** Adsorption of Congo Red Dye from Aqueous Solutions by Montmorillonite as a Low-cost Adsorbent. *DE GRUYTER: International Journal of Chemical Reactor Engineering*, 20160203, 1-11.
- Özcan, A. S. and Özcan, A. (2004).** Adsorption of acid dyes from aqueous solutions onto acid-activated bentonite. *Journal of Colloid and Interface Science*, 276, 39–46.
- Ozdes, D.; C. Duran; H. B. Senturk. (2011).** Adsorptive removal of Cd(II) and Pb(II) ions from aqueous solutions by using Turkish illitic clay. *Journal of Environmental Management*, 92, 3082-3090.
- Panda, A. K.; B. G. Mishra; D. K. Mishra and R. K. Singh. (2010).** Effect of sulphuric acid treatment on the physico-chemical characteristics of kaolin clay. *Colloids and Surfaces A: Physicochemical and Engineering Aspects*, 363, 98–104.
- Pathania, D.; S. Sharma and P. Singh. (2017).** Removal of methylene blue by adsorption onto activated carbon developed from *Ficus carica* bast. *Arabian Journal of Chemistry*, 10, 1445–1451.
- Qin, H.; T. Hua; Y. Zhaia; N. Lua and J. Aliyeva. (2020).** Sonochemical synthesis of ZnS nanolayers on the surface of microbial cells and their application in the removal of heavy metals, *Journal of Hazardous Materials*, 400, (123161), 1-11.
- Rahmani, A.; H. Zavvar Mousavi and M. Fazli. (2010).** Effect of nanostructure alumina on adsorption of heavy metals. *Desalination*, 253, 94–100.
- Ramachandran, P.; R. Vairamuthu and S. Ponnusamy. (2011).** Adsorption Isotherms, Kinetics, Thermodynamics and Desorption Studies of Reactive Orange 16 on Activated Carbon Derived from *Ananascomosus* (L.). *ARPN Journal of Engineering and Applied Sciences*, 6(11), 15-26.
- Rao, R. A. K. and Khan, U. (2017).** Adsorption studies of Cu (II) on Boston fern (*Nephrolepis exaltata* Schott cv. *Bostoniensis*) leaves, *Applied Water Science*, 7, 2051–2061.
- Razzak, S. A.; M. O. Faruque; Z. Alsheikh; L. Alsheikhmohamad; D. Alkuroud; A. Alfayez; S. M. Zakir Hossain and M. M. Hossain. (2022).** A comprehensive review on conventional and biological-driven heavy metals removal from industrial wastewater, *Environmental Advances*, 7, 100168, 1-26.
- Resmi, G.; S. G. Thampi and S. Chandrakaran. (2012).** Removal of lead from wastewater by adsorption using acid-activated clay, *Environmental Technology*, 33, (3), 291-297.
- Sari, A. and Tuzen, M. (2014).** Cd(II) adsorption from aqueous solution by raw and modified kaolinite. *Applied Clay Science*, 88-89, 63-72.
- Sarma, G. K.; S. Sen Gupta and K. G. Bhattacharyya. (2019).** Removal of hazardous basic dyes from aqueous solution by adsorption onto kaolinite and acid-treated kaolinite: kinetics, isotherm and mechanistic study, *Springer Nature Applied Sciences*, 1, (211), 1-15.
- Saxena, A.; M. Bhardwaj; T. Allen; S. Kumar and R. Sahney. (2017).** Adsorption of heavy metals from wastewater using agricultural–industrial wastes as biosorbents, *Water Science*, 31, (2), 189-197.
- Sdiri, A.; T. Higashi; T. Hatta; F. Jamoussi and N. Tase. (2011).** Evaluating the adsorptive capacity of montmorillonitic and calcareous clays on the removal of several heavy metals in aqueous systems. *Chemical Engineering Journal*, 172, 37–46.
- Siyanbola, T.; K. O. Ajanaku; O. O. James and J. A. Olugbuyiro. (2011).** Physico-Chemical Characteristics of Industrial Effluents In Lagos State, Nigeria. *G. J. P&A Sc and Tech.*, 1, 49-54.
- Sukpreabprom, H.; A. Arquero; W. Naksata; P. Sooksa and S. Janhom. (2014).** Isotherm, Kinetic and Thermodynamic Studies on the Adsorption of Cd (II) and Zn (II) ions from Aqueous Solutions onto Bottom Ash.

International Journal of Environmental Science and Development, 5 (2), 165-170.

Uddin, M. K. (2017). A review on the adsorption of heavy metals by clay minerals, with special focus on the past decade. *Chemical Engineering Journal* 308, 438–462.

Unuabonah, E. I.; B. I. Olu-Owolabi; K. O. Adebowale and I. Z. Yang. (2008). Removal of Lead and Cadmium Ions from Aqueous Solution by Polyvinyl alcohol-modified Kaolinite Clay: A Novel Nano-clay Adsorbent. *Adsorption Science & Technology*, 26 (6), 383-405.

Ye, C. and Fu, F. (2019). Behaviors of Structural Fe (II) of Nontronite and Aqueous Fe(II) on Cr(VI) Removal in the Presence of Citrate, *Water, Air, and Soil Pollutants*, 230, (288), 1-11.

Yin, J.; C. Deng; Z. Yu; X. Wang and G. Xu. (2018). Effective Removal of Lead Ions from Aqueous Solution Using Nano Illite/Smectite Clay: Isotherm, Kinetic, and Thermodynamic Modeling of Adsorption, *Water*, 10, (210), 1-13.